

A Review of the Theory and Applications of Optimal Subband and Transform Coders¹

P. P. Vaidyanathan and Sony Akkarakaran

Department of Electrical Engineering, California Institute of Technology, Pasadena, California 91125
E-mail: ppvnath@sys.caltech.edu, sony@systems.caltech.edu

The problem of optimizing digital filter banks based on input statistics was perhaps first addressed nearly four decades ago by Huang and Schultheiss. These authors actually considered a special case, namely transform coder optimization. Many of the subband coder optimization problems considered in recent years have close similarities to this work, though there are fundamental differences as well. Filter banks are used today not only for signal compression, but have found applications in signal denoising and in digital communications. A recent result is that principal component filter banks (PCFBs) offer an optimal solution to many problems under certain theoretical assumptions. While this result is quite powerful and includes several earlier results as special cases, there still remain some open problems in the area of filter bank optimization. We first give a review of the older classical methods to place the ideas in the right perspective. We then review recent results on PCFBs. The generality of these results is demonstrated by showing an application in digital communications (the discrete multitone channel). We show, for example, that the PCFB minimizes transmitted power for a given probability of error and bit rate. Future directions and open problems are discussed as well.

© 2001 Academic Press

1. INTRODUCTION

The optimization of filter banks based on knowledge of input statistics has been of interest for a long time. The history of this problem goes back to the pre-filter-bank days when Huang and Schultheiss [27] published fundamental results on the optimization of transform coders under fairly general conditions, nearly four decades ago (Subsection 3.1). Since then the signal processing community has made many advances in the theory of filter banks, wavelets, and their applications. In particular there has been significant progress in the optimization of filter banks for various applications including signal compression, signal denoising, and digital communications. One of the most recent results in this field is that a type of filter bank called the principal component filter bank (PCFB) offers an optimal solution to many problems under fairly mild theoretical

¹ Work supported in part by the NSF Grant MIP 0703755, ONR Grant N00014-99-1-1002, and Microsoft Research, Redmond, WA.

assumptions. While this result is in itself powerful and includes several earlier results as special cases, there still remain many open problems in the area of filter bank optimization.

In this paper we first give a review of the older “classical approaches” to filter bank optimization, to place the ideas in the right perspective. We then review more recent results on optimal filter banks. This includes a review of principal component filter banks, their optimality properties, and some applications of these. To emphasize the generality of these results we show an application in digital communications (the discrete multitone channel). We show, for example, that the PCFB minimizes transmitted power for a given probability of error and bit rate. We finally discuss future directions and open problems in this broad area.

1.1. Standard Notations

Most notations are as in [62]. The device denoted as $\downarrow M$ in Fig. 1a denotes the M -fold decimator and $\uparrow M$ denotes the M -fold expander. Similarly we use the notations $[x(n)]_{\downarrow M}$ and $[X(z)]_{\downarrow M}$ to denote the decimated version $x(Mn)$ and its z -transform. The expanded version

$$\begin{cases} x(n/M), & n = \text{mul. of } M, \\ 0, & \text{otherwise} \end{cases}$$

is similarly denoted by $[x(n)]_{\uparrow M}$, and its z -transform $X(z^M)$ is denoted by $[X(z)]_{\uparrow M}$. In general the filters are allowed to be ideal (e.g., brickwall lowpass, etc.). So the z -transforms do not necessarily exist. The notation $H(z)$ should be regarded as an abbreviation for the Fourier transform $H(e^{j\omega})$.

1.2. Background Material and Terminology

Figure 1a shows the standard M -channel filter bank which can be found in many signal processing books, e.g., [4, 40, 62, 71]. The subband processors P_i are typically quantizers but as we shall see later, they can represent other kinds of nonlinear or linear operations such as a hard threshold device, a linear multiplier, and so forth. This is said to be a **uniform** filter bank because all the decimators are identical. All our discussions are for uniform filter banks. Using the polyphase notations described, for example, in [62, Chap. 5], we can redraw the uniform filter bank in the form shown in Fig. 1b. The system shown in Fig. 1a is said to be a **biorthogonal** system if the filters are such that the matrix $\mathbf{R}(e^{j\omega})$ is the inverse of $\mathbf{E}(e^{j\omega})$ for all ω . This is also called the perfect reconstruction property or **PR property**. The reason is that in absence of any subband processing, this implies $\hat{x}(n) = x(n)$ for all n .

For the special case where the matrices $\mathbf{E}(z)$ and $\mathbf{R}(z)$ are constants, the system of Fig. 1 is said to be a **transform coder**.² The set of M filters $\{H_k(z)\}$ is said to be **orthonormal** if the polyphase matrix $\mathbf{E}(e^{j\omega})$ is unitary for all ω . Such a transfer matrix $\mathbf{E}(z)$ is said to be **paraunitary**. Orthonormal filter banks are therefore also known as paraunitary filter banks. In this case biorthogonality is achieved by choosing the synthesis

² There is a viewpoint that the distinction between the subband and transform coder is “artificial,” especially in the way they are implemented today; see [48].

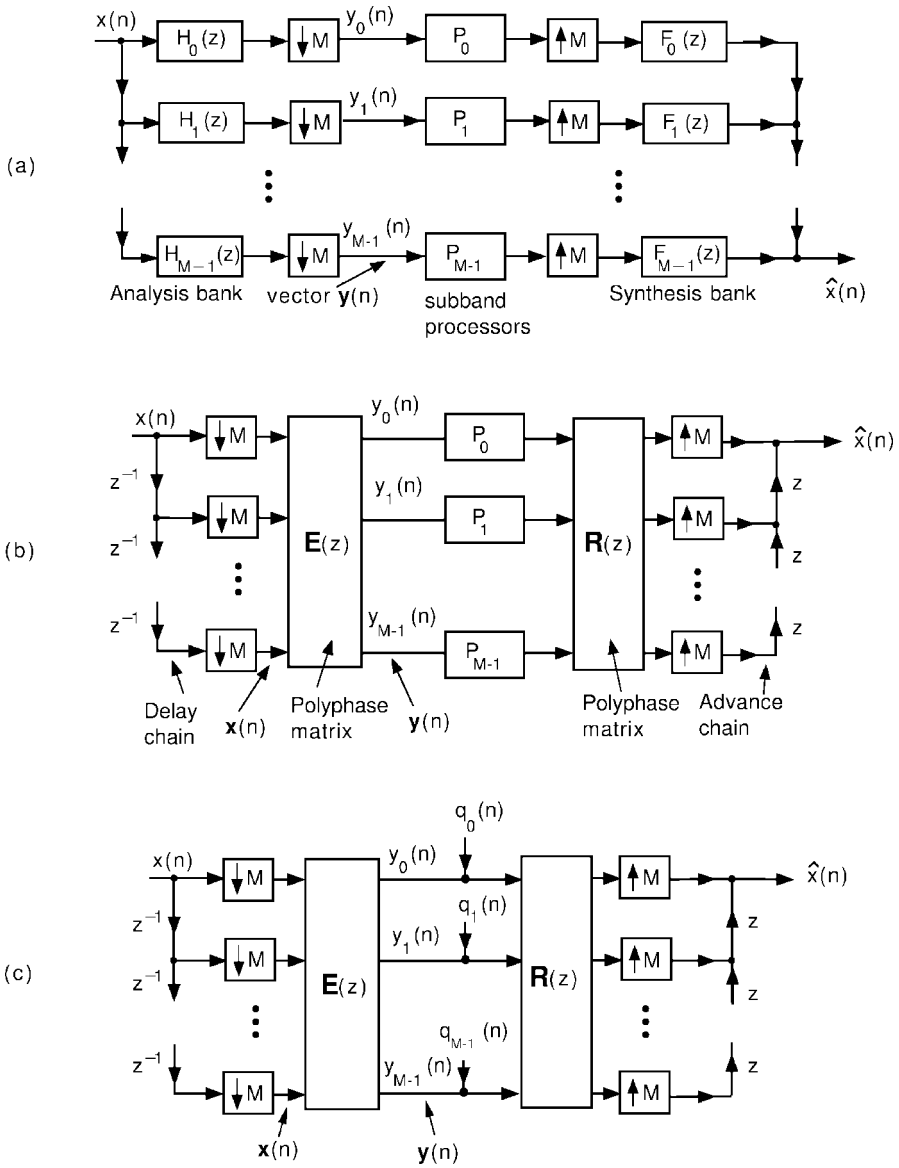


FIG. 1. (a) The M -channel maximally decimated filter bank with uniform decimation ratio M , (b) its polyphase representation, and (c) additive noise model.

filters to be $F_k(e^{j\omega}) = H_k^*(e^{j\omega})$. Figure 2 shows two extreme examples of orthonormal filter banks. In the first example the filters are trivial delay elements $H_k(z) = z^{-k}$ and $F_k(z) = z^k$; this is called the **delay chain system**. In the second example the filters are ideal nonoverlapping (unrealizable) bandpass filters; this is called the ideal **brickwall** filter bank with contiguous stacking. It can be shown that the biorthogonality property is equivalent to the condition

$$H_k(e^{j\omega})F_m(e^{j\omega})\Big|_{\downarrow M} = \delta(k - m).$$

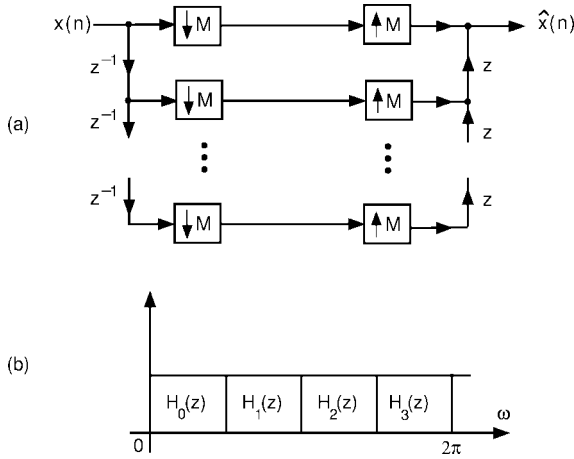


FIG. 2. Examples of orthonormal filter banks. (a) The delay chain system, and (b) the brickwall filter bank with contiguous stacking.

For the case of orthonormal filter banks this yields $H_k(e^{j\omega})H_m^*(e^{j\omega})|_{\downarrow M} = \delta(k - m)$. Thus, each filter satisfies

$$|H_k(e^{j\omega})|_{\downarrow M}^2 = 1 \quad (\text{Nyquist constraint})$$

which is equivalent to

$$\sum_{m=0}^{M-1} |H_k(e^{j(\omega - 2\pi m/M)})|^2 = M, \quad \text{for all } \omega. \quad (1)$$

This constraint implies the **unit-energy** property $\int_0^{2\pi} |H_k(e^{j\omega})|^2 d\omega/2\pi = 1$ as well as the **boundedness** property $|H_k(e^{j\omega})|^2 \leq M$. These properties hold for the synthesis filters $F_k(e^{j\omega})$ as well. If the impulse response of $|H_k(e^{j\omega})|^2$ is denoted as $g_k(n)$ then the preceding Nyquist condition is equivalent to $g_k(Mn) = \delta(n)$. That is, $g_k(n)$ is zero at nonzero multiples of M .

1.3. Assumptions

Two standard assumptions often encountered in filter bank optimization problems are the wide sense stationary (WSS) assumption and the high bit-rate assumption. As explained in the paper, many of the recent results hold without these assumptions.

Wide sense stationary (WSS) assumption. Under this assumption the input $x(n)$ is a zero-mean WSS process with power spectral density or *psd* denoted as $S_{xx}(e^{j\omega})$. The decimated subband signals, denoted as $y_i(n)$ in Fig. 1, are therefore (zero-mean and) jointly WSS with variances denoted by σ_i^2 . The vector $\mathbf{x}(n)$ indicated in Fig. 1b is also WSS under this assumption. This vector is said to be the **blocked version** of $x(n)$. The WSS assumption is made throughout the paper unless stated otherwise.

High bit-rate assumption. The quantizer noise sources $q_k(n)$ are jointly WSS, white, and uncorrelated, with zero mean and variances given by [28; 62, Appendix C]

$$\sigma_{q_k}^2 = c\sigma_k^2 2^{-2b_k}, \quad (2)$$

where σ_k^2 is variance of the subband signal $y_k(n)$ and b_k is the number of bits assigned to the k th subband quantizer. Thus the noise decays exponentially with number of bits b_k . The constant c is implicitly assumed to be the same in all subbands. The main component of the high bit-rate assumption is the formula (2). The assumption is unsatisfactory in practice because the b_k are usually quite small in data compression applications. The assumption has recently been replaced with more satisfactory ones. For example, in Section 6 we prove the optimality of principal component filter banks without using this assumption.

1.4. Related Past Work

We present connections to past work at the beginning of various sections. Here is a broad overview. The optimal transform coder problem was formulated and solved by Huang and Schultheiss [27] nearly four decades ago. For the case of subband coders various useful cases of the filter bank optimization problem have been considered by a number of authors, for example, by Akansu and Liu [5], Haddad and Uzun [23], Tewfik *et al.* [55], Gopinath *et al.* [22], Malvar and Staelin [41], and Dasgupta *et al.* [15].

The optimality of principal component filter banks (PCFB) for certain objectives was observed independently by a number of authors [56, 60, 61, 73]. For the unconstrained class \mathcal{C}^u of orthonormal filter banks the PCFB was introduced by Tsatsanis and Giannakis [56]. The goal in that work was to construct a filter bank with minimum reconstruction error if a subset of subband signals are to be retained (see Section 6 for more precise details). A similar construction was also proposed independently by Unser [60] who also conjectured [61] that the PCFB might be optimal for a larger class of objectives, namely error measures of the form $\sum_i h(\sigma_i^2)$ where $h(\cdot)$ is concave. This conjecture is proved to be true in Mallat's book [39, Theorem 9.8, p. 398] using a result of Hardy *et al.* Independently, a set of necessary and sufficient conditions for maximization of coding gain was established in [66] and a systematic way to satisfy these conditions was developed. The result turned out to be identical to principal component filter banks obtained in [56] for a different objective. More recently the PCFB has been shown to be optimal for an even broader class of objectives [6, 9]. It covers many of the special cases reported earlier in the literature.

There exists plenty of other good literature which will not be part of our discussion here. The fact that reconstruction noise in filter banks is typically cyclostationary has been observed by several authors [46, 62]. A sound theoretical explanation of the merits of subband coding (with ideal brickwall filters) was given by Rao and Pearlman [50] for the pyramid structure, and further results along those lines have been reported by Fischer [19] and de Queiroz and Malvar [16]. The design of optimal signal-adapted filter banks for FIR and IIR cases has also been addressed by Moulin *et al.* [42, 43] who also show how the results extend for the biorthogonal case. Several important results in this direction can be found in [44].

1.5. Scope and Outline

Most of this paper is restricted to the case of uniform orthonormal filter banks. In Section 2 we give an overview of situations where principal component filter banks arise. Section 3 is a review of standard classical approaches to filter bank optimization. This includes transform coders as well as ideal subband coders. A brief description of compaction filters which arise in this context is given in Section 4. In Section 5 we supply the mathematical background required to understand the more recent theory of principal component filter banks (PCFB). Sections 6–9 give a complete treatment of the PCFB and its optimality properties. The application of PCFB in the design of optimal multitone communication systems (DMT systems) is discussed in Section 10 after a brief introduction to DMT systems. There are many related problems and results which are not discussed in this paper. An important part in the design of optimal orthonormal filter banks is the design of energy compaction filters. This has been addressed in great detail in [33, 58]. In this paper we do not discuss compaction filters in detail, nor do we consider the optimization of **biorthogonal** filter banks. The interested reader can pursue a number of key references cited in [67].

2. OVERVIEW OF SITUATIONS WHERE PRINCIPAL COMPONENT FILTER BANKS ARISE

We will define principal component filter banks or **PCFBs** only in Section 6. But it is convenient to mention at the outset some problems for which such filter banks are optimal. Suppose the subband processor P_i (which we have not specified yet) introduces an additive error $q_i(n)$ as indicated in Fig. 1c. Let $q_i(n)$ be zero-mean random variables with variance $\sigma_{q_i}^2$. Assuming the filter bank is orthonormal (Subsection 1.2) we can show that the reconstruction error $e(n) \triangleq \hat{x}(n) - x(n)$ has average variance

$$\sigma_e^2 = \frac{1}{M} \sum_{i=0}^{M-1} \sigma_{q_i}^2.$$

This follows from orthonormality and is true even if $q_i(n)$ are not white and uncorrelated [62]. The following are some examples of problems where the PCFB arises.

EXAMPLE 1. If P_i are high bit-rate quantizers (Subsection 1.3) then the reconstruction error is $\sigma_e^2 = \sum_i c_i 2^{-2b_i} \sigma_i^2 / M$. Assuming that c_i are identical for all i and independent of the choice of filters, and that optimal bit allocation [62] has been performed, it was shown in [66] that the filter bank which minimizes σ_e^2 is a PCFB.

EXAMPLE 2. The preceding result was shown later to be true under less restricted assumptions. Indeed, assume that the subband processors P_i are quantizers with normalized **distortion rate functions** $f_i(b_i) > 0$ (with b_i denoting the rate). This means $\sigma_{q_i}^2 = f_i(b_i) \sigma_i^2$ and the reconstruction error is $\sigma_e^2 = \sum_i f_i(b_i) \sigma_i^2 / M$. For example, $f_i(b_i)$ could represent **low bit rate** quantizers violating standard high bit rate assumptions. It was

shown recently [32] that as long as $f_i(\cdot)$ and b_i do not depend³ on the filters $H_i(z)$, the filter bank which minimizes σ_e^2 is still a PCFB.

EXAMPLE 3. The optimality of the PCFB holds even if the subband processors P_i are “keep or kill” systems. Such a system keeps P dominant bands and throws away the rest (in fact this was the origin of the PCFB concept [56]).

More recently it has been shown [9] that the PCFB is optimal for an even broader class of problems for which the objective function can be expressed as a **concave function** of the subband variance vector

$$\mathbf{v} = [\sigma_0^2 \ \sigma_1^2 \ \dots \ \sigma_{M-1}^2]^T. \quad (3)$$

For example, suppose the input $x(n)$ is a **signal buried in noise** and the purpose of the filter bank is to produce a better signal-to-noise ratio. In this case the subband processors P_i could be **Wiener filters**, or they could be **hard threshold** devices (as in denoising [18]). In these cases the objective to be minimized is the (mean square) noise component in the filter bank output. With suitable assumptions on the signal and noise statistics, this problem can be formulated as the minimization of a concave function of the subband variances, and the solution is still a PCFB. The same theoretical tool can also be used to prove the optimality of PCFB in digital communications. For example, the PCFB minimizes transmitted power for a given bit rate and error probability in discrete multitone communications (Section 10).

3. REVIEW OF PAST WORK ON OPTIMAL TRANSFORM AND SUBBAND CODERS

In this section we review some of the early approaches to the optimization of transform and subband coders. Past results on optimal transform coders are reviewed first, followed by work on optimal subband coders. This adds insight and places the most recent results in the proper historical perspective.

3.1. Optimal Transform Coders

In their pioneering 1963 paper Huang and Schultheiss proved a number of results for the transform coder system [27]. The scheme they considered is shown in Fig. 3. This can be regarded as a special case of Fig. 1b when $\mathbf{E}(z)$ and $\mathbf{R}(z)$ are constant matrices. Equivalently, the filters $H_k(z)$ and $F_k(z)$ are FIR with length $\leq M$. Notice however that the components $x_k(n)$ do not necessarily come from a scalar input $x(n)$ as in Fig. 1b. In fact the time argument (n) is not present in the discussions in [27] and will be temporarily deleted here as well.

The authors of [27] make the following assumptions:

(1) The input to \mathbf{E} is a real Gaussian random vector $\mathbf{x} = [x_0 \ x_1 \ \dots \ x_{M-1}]^T$ with zero mean and autocorrelation $\mathbf{C}_{xx} = E[\mathbf{xx}^T]$.

³ This assumption is sometimes true; for example, if $x(n)$ is Gaussian then the quantizer inputs are also Gaussian regardless of $H_i(z)$, and $f_i(b_i)$ are independent of $H_i(z)$.

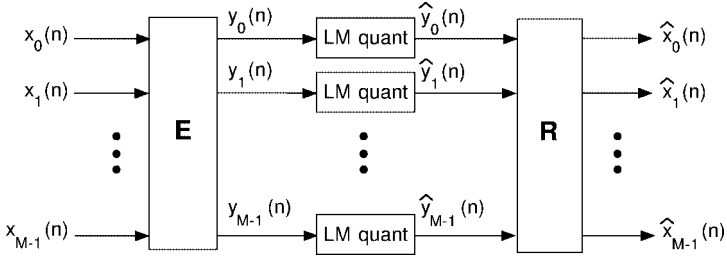


FIG. 3. The transform coder scheme for vector signals.

(2) \mathbf{E} is a real nonsingular matrix diagonalizing the covariance matrix of its input. The random variables y_k and y_m are therefore uncorrelated for $k \neq m$ (and independent, by joint Gaussianity).⁴

(3) The subband processors P_k are b_k -bit optimal Lloyd–Max quantizers [21]. These quantizers have a certain **orthogonality property**. Namely, the quantized result \hat{y}_k is orthogonal to the quantization error $q_k = y_k - \hat{y}_k$, that is, $E[q_k \hat{y}_k] = 0$. This assumption is crucial to some of the proofs given in [27]. Notice that there is no high bit-rate assumption.

(4) The subbands are numbered such that the variances of y_k are in decreasing order, that is, $\sigma_0^2 \geq \sigma_1^2 \geq \sigma_2^2 \geq \dots$. The number of bits are also ordered such that $b_0 \geq b_1 \geq b_2 \geq \dots$. The average $b = \sum_i b_i / M$ is fixed.

Under these assumptions the authors seek to minimize the reconstruction error $\sum_{k=0}^{M-1} E[(\hat{x}_k - x_k)^2]$. It is shown that the best reconstruction matrix \mathbf{R} is the inverse of \mathbf{E} . That is, the best system is **biorthogonal**. It is also shown that if we further choose to optimize \mathbf{E} , then it should be a unitary matrix whose rows are eigenvectors of the input covariance matrix. This \mathbf{E} is said to be the Karhunen Loeve transform or **KLT** of the input vector \mathbf{x} . In short, the optimal system can be restricted to be an *orthonormal* filter bank with \mathbf{E} chosen as the KLT of the input. Finally if we choose to do so, we can further optimize the allocation of bits b_k . The authors also obtain an expression for optimal bit allocation b_k . This, however, might yield noninteger values. If b_k are large we can approximate these with integers, but for small b this may not be true; in fact some of the b_k might turn out to be negative.

In a 1976 paper, Segall generalized these results in many ways [52]. For example, the bits b_k are constrained to be nonnegative integers in the optimization. It was shown that the best synthesis matrix \mathbf{R} is the inverse of \mathbf{E} only for the special case of Lloyd–Max quantizers (which have the orthogonality property explained above). More generally $\mathbf{R}(z)$ is a product of \mathbf{E}^{-1} with a **Wiener filter** matrix. In fact even when $\mathbf{E}(z)$ is not a constant, such a result has been proved in [64]. Namely, the best $\mathbf{R}(z)$ is in general $\mathbf{E}^{-1}(z)$ followed by a Wiener filter which depends on the statistics of the subband signals and subband errors.⁵ The Wiener matrix reduces to identity when optimal vector quantizers are used in each of the subbands. Except in this case, **biorthogonality is a loss of generality**. Since

⁴ That is, \mathbf{C}_{yy} is diagonal. The autocorrelations are related by $\mathbf{C}_{yy} = \mathbf{E}\mathbf{C}_{xx}\mathbf{E}^\dagger$. Since this is a congruence rather than a similarity transformation, the diagonal elements of \mathbf{C}_{yy} are not necessarily the eigenvalues of \mathbf{C}_{xx} (unless \mathbf{E} is unitary).

⁵ A thorough study of this can be found in the later work [24].

the Wiener matrix depends on the statistics of the signal it is often difficult to implement. Biorthogonal filter banks and the special case of orthonormal filter banks are therefore more attractive in practice. In this paper we concentrate only on orthonormal filter banks.

The mathematical methods used in [27] are quite sophisticated. However, the results given in [27] can be proved in a more elementary way if the subband quantizers satisfy the high bit-rate assumption (Subsection 1.3). For example, the optimality of the KLT matrix follows rather trivially under this assumption [28, 62]. Thus the advantage of the high bit-rate assumption, in theory, is that it makes the derivations simpler, and often provides insight.

3.2. Optimal Subband Coders

In general the term subband coder is used when $\mathbf{E}(z)$ is not a constant but a function of z . The transform coder is therefore a special case. For subband coders, the optimality problem becomes more complicated because $\mathbf{E}(e^{j\omega})$ should now be specified for all ω . Theoretical results paralleling the transform coder results of Huang, Schultheiss, and Segall are therefore not easily obtained. The result to be reviewed here is insightful in the sense that it brings principal component filter banks into the picture rather naturally by deriving necessary and sufficient conditions for optimality of uniform orthonormal subband coders. Actually the results reviewed here only assume that the quantizer variances are given by the formula (2), even though $q_i(n)$ need not be white and uncorrelated [66]. This section considers the case where the filters have unrestricted order (e.g., ideal brickwall filters are allowed).

Assume that the **average bit rate** $b = \sum_{i=0}^{M-1} b_i/M$ is fixed. The coding gain of a subband coder is defined as

$$G_{SBC}(M) \triangleq \frac{\mathcal{E}_{direct}}{\mathcal{E}_{SBC}},$$

where \mathcal{E}_{SBC} is the mean square value of the reconstruction error $\hat{x}(n) - x(n)$, and \mathcal{E}_{direct} is the m.s. value of the direct quantization error (roundoff quantizer [28, 47]) with the same bit-rate b . Using the high bit-rate model (Subsection 1.3) the coding gain $G_{SBC}(M)$ of the uniform orthonormal subband coder is (e.g., see [62, Appendix C])

$$G_{SBC}(M) = \frac{\sum_{i=0}^{M-1} \sigma_i^2/M}{(\prod_{i=0}^{M-1} \sigma_i^2)^{1/M}} = \frac{\sigma_x^2}{(\prod_{i=0}^{M-1} \sigma_i^2)^{1/M}}. \quad (4)$$

Here we have used $\sum_{i=0}^{M-1} \sigma_i^2 = M\sigma_x^2$, which is valid for uniform orthonormal filter banks. The preceding coding gain expression assumes *optimal bit allocation*.⁶ Equation (4) represents the ratio of the arithmetic and geometric means (AM/GM ratio) of the subband variances σ_i^2 . Maximizing this ratio is equivalent to minimizing the product of subband variances $\prod_{i=0}^{M-1} \sigma_i^2$. For fixed input psd $S_{xx}(e^{j\omega})$ these variances σ_i^2 depend only on the analysis filters $H_i(e^{j\omega})$.

Total decorrelation. In orthogonal transform coding theory where $\mathbf{E}(z)$ in Fig. 1b is a constant unitary matrix, it is known that subband decorrelation ($E[y_i(n)y_k^*(n)] = 0$,

⁶ In this paper we do not consider details of optimal bit allocation. Some details can be found in [28, 62].

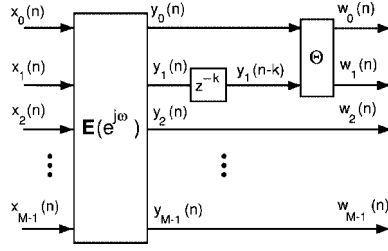


FIG. 4. Proof that total decorrelation is necessary.

$i \neq k$) is necessary and sufficient for maximization of the coding gain (4) [28, 62]. For orthonormal subband coders, a stronger condition is necessary, namely

$$E[y_i(n)y_k^*(m)] = 0 \quad (5)$$

for $i \neq k$, and for all n, m . This condition will also be referred to as **total decorrelation** of subbands. This condition follows from the fact that if a pair of decimated subband processes, say $y_0(\cdot)$ and $y_1(\cdot)$, are not uncorrelated, then we can insert a delay z^{-k} and a unitary matrix Θ to transform the pair $y_0(n), y_1(n-k)$ into an uncorrelated pair $w_0(n), w_1(n)$ (Fig. 4). It can be shown that $\sigma_{w_0}^2 \sigma_{w_1}^2 < \sigma_0^2 \sigma_1^2$, so the *AM/GM* ratio (4) can be increased.

Spectral majorization. Total decorrelation, while necessary, is not sufficient for maximization of (4). For example, the traditional brickwall subband coder in Fig. 2b satisfies this condition for any input psd because the filters are nonoverlapping. It can be shown that a condition called spectral majorization is also necessary. We say that the set of decimated subband signals $y_k(n)$ has the spectral majorization property if their power spectra $\{S_k(e^{j\omega})\}$ satisfy (see Fig. 5a)

$$S_0(e^{j\omega}) \geq S_1(e^{j\omega}) \geq \dots \geq S_{M-1}(e^{j\omega}), \quad \text{for all } \omega, \quad (6)$$

where the subbands are numbered such that $\sigma_i^2 \geq \sigma_{i+1}^2$. If condition (6) is not satisfied, we can cascade a frequency dependent permutation matrix $\mathbf{T}(e^{j\omega})$ (which is unitary) as shown in Fig. 5b and increase the *AM/GM* ratio (4) [66]. This shows that spectral majorization property is a necessary condition.

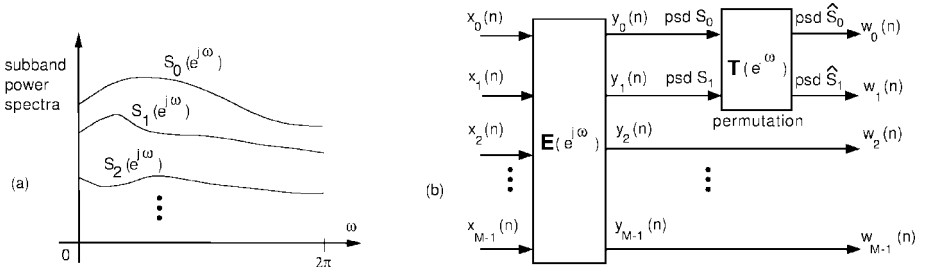


FIG. 5. (a) Example of majorized subband spectra, and (b) proof that spectral majorization is necessary.

Though spectral majorization and total decorrelation are necessary for optimality, neither of them is individually sufficient. For example, the brickwall subband coder with contiguous stacking (Fig. 2b) satisfies the total decorrelation property for any input psd. On the other hand the delay chain system of Fig. 2a satisfies spectral majorization for any input, though it yields no coding gain! It turns out, however, that total decorrelation and spectral majorization, imposed together, become very powerful [66]:

THEOREM 1 (A Necessary and Sufficient Condition for Optimality). *Consider the uniform orthonormal subband coder with unlimited filter orders. For fixed input psd $S_{xx}(e^{j\omega})$, the AM/GM ratio (4) (coding gain under high bit-rate assumption) is maximized if and only if the decimated subband signals $y_k(n)$ simultaneously satisfy total decorrelation and spectral majorization. Furthermore, when these conditions are satisfied, the set of power spectra $\{S_k(e^{j\omega})\}$ of the decimated subband signals is unique.*

A proof can be found in [66]. Notice that the analysis filters of the optimal system may not be unique because the diagonalizing eigenvector matrix may not be unique. Given an input power spectrum $S_{xx}(e^{j\omega})$ an orthonormal filter bank $\{H_k(z)\}$ satisfying the optimality conditions of Theorem 1 can be designed using a standard procedure described in [66]. This procedure requires the idea of an optimal compaction filter, reviewed next.

4. COMPACTION FILTERS AND OPTIMAL FILTER BANKS

Figure 6 shows a filter $H(e^{j\omega})$ with a zero-mean WSS input $x(n)$ having psd $S_{xx}(e^{j\omega})$. Consider the problem of designing $H(e^{j\omega})$ such that the output variance σ_y^2 is maximized subject to the constraint that $|H(e^{j\omega})|^2$ be **Nyquist(M)** (Subsection 1.2). The solution $H(e^{j\omega})$ is called an optimum **compaction(M) filter**, and the ratio σ_y^2/σ_x^2 the **compaction gain**. The Nyquist constraint is imposed because it has to be satisfied for filters in orthonormal filter banks. The following is a refined version for arbitrary M , of Unser’s construction of compaction filters [60]: (a) For each frequency ω_0 in $0 \leq \omega < 2\pi/M$ define the M alias frequencies $\omega_k = \omega_0 + 2\pi k/M$, where $0 \leq k \leq M - 1$. (b) Compare the values of $S_{xx}(e^{j\omega})$ at these M alias frequencies $\{\omega_k\}$. Let L be the smallest integer such that $S_{xx}(e^{j\omega_L})$ is a maximum in this set. Then assign

$$H(e^{j(\omega_0 + (2\pi k/M))}) = \begin{cases} \sqrt{M} & \text{when } k = L \\ 0 & \text{otherwise.} \end{cases} \tag{7}$$

Repeating this for each ω_0 in the region $0 \leq \omega < 2\pi/M$, the filter $H(e^{j\omega})$ is completely defined for all ω in $0 \leq \omega < 2\pi$. This filter maximizes the output variance σ_y^2 under the Nyquist(M) constraint.

Properties. If $H(e^{j\omega})$ is an optimal compaction(M) filter for an input psd $S_{xx}(e^{j\omega})$ then it will be a valid optimal solution for the modified psd $f[S_{xx}(e^{j\omega})]$ where $f[\cdot] \geq 0$

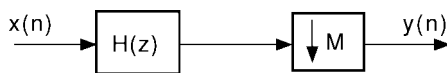


FIG. 6. The compaction filter.

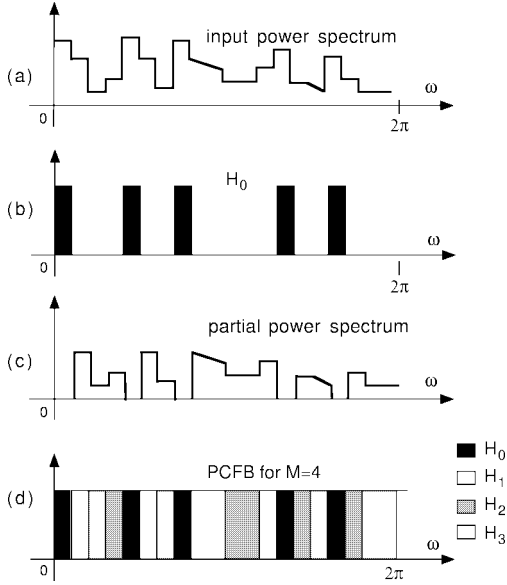


FIG. 7. (a) Example of an input power spectrum $S_{xx}(e^{j\omega})$, (b), (c) explanation of the construction of filters in the four channel orthonormal filter bank, and (d) the filter bank which maximizes the AM/GM ratio (4).

is any nondecreasing function. If a psd is nonincreasing in $[0, 2\pi)$, then the optimum compaction filter is **lowpass**. While the optimal compaction filter is not unique, the construction described above yields an ideal **two-level filter** with passband response $= \sqrt{M}$ and stopband response equal to zero. The total width of all passbands is $2\pi/M$.

To describe the construction of filter banks which maximize the AM/GM ratio (4), consider the example of input psd shown in Fig. 7a, and let $M = 4$. The first step is to choose one filter, $H_0(e^{j\omega})$, to be an optimal energy compaction filter for $S_{xx}(e^{j\omega})$ (Fig. 7b). Let the passband support of $H_0(e^{j\omega})$ be denoted \mathcal{S}_0 . Define a “partial” psd

$$S_{xx}^{(1)}(e^{j\omega}) = \begin{cases} 0 & \text{for } \omega \in \mathcal{S}_0 \\ S_{xx}(e^{j\omega}) & \text{otherwise,} \end{cases} \quad (8)$$

as shown in Fig. 7c. Thus $S_{xx}^{(1)}(e^{j\omega})$ is obtained by **peeling off** the portion of $S_{xx}(e^{j\omega})$ falling in the passband of $H_0(e^{j\omega})$. Design the next analysis filter $H_1(e^{j\omega})$ to be the optimal compaction filter for $S_{xx}^{(1)}(e^{j\omega})$. Define the next partial psd $S_{xx}^{(2)}(e^{j\omega})$ by peeling off the portions of $S_{xx}(e^{j\omega})$ in the passbands of $H_0(e^{j\omega})$ and $H_1(e^{j\omega})$, and continue in this manner. Thus all the analysis filters can be identified (part (d) in the figure). Since the filters are nonoverlapping, total decorrelation is satisfied. Moreover it can be shown that spectral majorization is satisfied by this construction [66]. It follows therefore that the filter bank maximizes the ratio (4). Filters constructed according to this algorithm are ideal infinite order filters. If we approximate these with FIR filters we get good approximations of the theoretical coding gain.

If the preceding algorithm is used to design an optimal filter bank for a **monotone** decreasing or increasing power spectrum, then the result is the traditional **brickwall** filter bank.

5. MATHEMATICAL PRELIMINARIES FOR PCFB THEORY

We now review mathematical results which will be useful in the theory of principal component filter banks. While some of these will be familiar to many readers, there are several that are not frequently used in the signal processing literature.

5.1. Convex Polytopes and Concave Functions

A linear combination of the form $\sum_{i=1}^N \alpha_i \mathbf{v}_i$ where $\alpha_i \geq 0$ and $\sum_i \alpha_i = 1$ is called a **convex combination** of the N vectors $\{\mathbf{v}_i\}$. A set \mathcal{D} of vectors is said to be a **convex set** if all convex combinations of vectors in \mathcal{D} still belong to \mathcal{D} . Figure 8 shows examples of convex and nonconvex sets. Let \mathcal{S} be a convex set of vectors. We say that $\mathbf{c} \in \mathcal{S}$ is an **extreme point** of \mathcal{S} if it cannot be written as a nontrivial convex combination of members in \mathcal{S} . That is, if $\mathbf{c} = \sum \alpha_i \mathbf{w}_i$ for distinct $\mathbf{w}_i \in \mathcal{S}$ and $\alpha_i \geq 0$ with $\sum_i \alpha_i = 1$, then $\alpha_i = 1$ for some i and zero for all other i . Figure 8 also indicates examples of extreme points. Note that in Fig. 8a all the boundary points are extreme points.

Next, let $f(\mathbf{v})$ be a real valued function of the vector $\mathbf{v} \in \mathcal{D}$ where the domain \mathcal{D} is a convex set. We say that $f(\mathbf{v})$ is *concave* on \mathcal{D} if

$$f(\alpha \mathbf{v}_1 + (1 - \alpha) \mathbf{v}_2) \geq \alpha f(\mathbf{v}_1) + (1 - \alpha) f(\mathbf{v}_2)$$

for every $\mathbf{v}_1, \mathbf{v}_2 \in \mathcal{D}$ and for every α such that $0 \leq \alpha \leq 1$. Geometrically, the function lies above the **chord connecting** any two points. We say $f(\mathbf{v})$ is a **convex function** if $-f(\mathbf{v})$ is concave.

Examples and properties. e^t and e^{-t} are convex whereas $\log t$ is concave. The function $f(t) = t$ is both convex and concave. If $f(\mathbf{v})$ is concave in \mathbf{v} then so is $cf(\mathbf{v})$ for $c \geq 0$. Similarly the sum of concave functions is concave. More generally, let $f(\mathbf{v})$ and $g(\mathbf{u})$ be concave functions where \mathbf{v} and \mathbf{u} are vectors of possibly different sizes. Define $h(\mathbf{w}) = f(\mathbf{v}) + g(\mathbf{u})$ where $\mathbf{w} = [\mathbf{v}^T \ \mathbf{u}^T]^T$. Then we can verify that $h(\mathbf{w})$ is concave in \mathbf{w} . If all the second partial derivatives $\partial^2 f / \partial v_i \partial v_j$ exist we can check convexity by looking at the Hessian matrix with elements $[\partial^2 f / \partial v_i \partial v_j]$. Thus $f(\mathbf{v})$ is convex if and only if this matrix is positive semidefinite [20] (e.g., second derivative nonnegative in the scalar case).

The definitions of concave and convex functions make sense only if the domain is a convex set, for otherwise, $\alpha \mathbf{v}_1 + (1 - \alpha) \mathbf{v}_2$ may not be in the domain. If the domain \mathcal{S} is not convex we often create a convex set \mathcal{D} containing \mathcal{S} and then take it to be the domain. Given an arbitrary set of vectors \mathcal{S} , its **convex hull**, denoted by $co(\mathcal{S})$, is the intersection

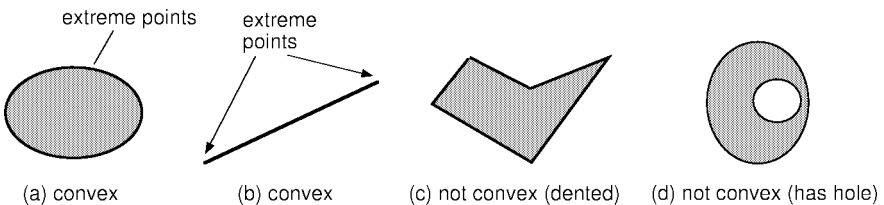


FIG. 8. Examples of convex and nonconvex sets in two dimensions. Parts (a) and (b) are convex whereas (c) and (d) are not.

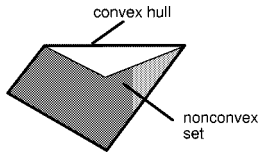


FIG. 9. A nonconvex set and its convex hull.

of all convex sets containing \mathcal{S} . Figure 9 shows the example of a nonconvex set and its convex hull.

DEFINITION 1. Convex Polytopes. Let $\{\mathbf{v}_1, \mathbf{v}_2, \dots, \mathbf{v}_N\}$ be a finite set of distinct vectors and \mathcal{P} the set of their convex combinations, i.e., vectors of the form $\sum_{i=1}^N \alpha_i \mathbf{v}_i$, with $\alpha_i \geq 0$ and $\sum_i \alpha_i = 1$. This can be verified to be a convex set and is therefore the convex hull of the finite set $\{\mathbf{v}_i\}$. We call \mathcal{P} the convex polytope generated by $\{\mathbf{v}_i\}$. Figure 10 shows examples. If the generating vectors \mathbf{v}_i are permutations of each other, then we refer to \mathcal{P} as a **permutation-symmetric** polytope.

LEMMA 1 (Generating Vectors Are Extreme Points). *Assuming that the generating set $\{\mathbf{v}_i\}$ is minimal (no \mathbf{v}_i is a convex combination of the others), the vectors \mathbf{v}_i are extreme points (in the sense defined at the beginning of this section) of the polytope \mathcal{P} . This is clear from pictures of polytopes such as the ones shown in Figure 10. For a more formal proof see Appendix A.*

5.2. Majorization Theory

Let $A = \{a_0, a_1, \dots, a_{M-1}\}$ and $B = \{b_0, b_1, \dots, b_{M-1}\}$ be two sets of real numbers. The set A is said to **majorize** the set B if, after reordering such that $a_0 \geq a_1 \geq a_2 \geq \dots$, and $b_0 \geq b_1 \geq b_2 \geq \dots$, we have

$$\sum_{i=0}^P a_i \geq \sum_{i=0}^P b_i$$

for $0 \leq P \leq M - 1$, and moreover, $\sum_{i=0}^{M-1} a_i = \sum_{i=0}^{M-1} b_i$. Thus every partial sum of the first set is at least as large as the corresponding partial sum of the second set. Defining the column vectors

$$\mathbf{a} = [a_0 \ a_1 \ \dots \ a_{M-1}]^T \quad \text{and} \quad \mathbf{b} = [b_0 \ b_1 \ \dots \ b_{M-1}]^T$$

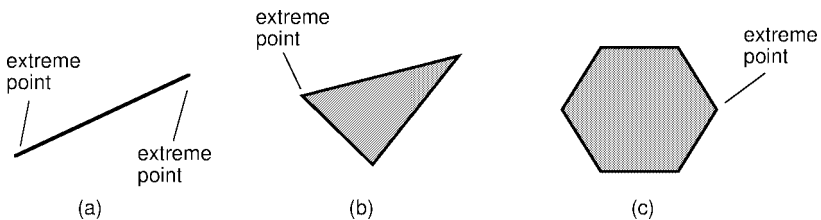


FIG. 10. Examples of convex polytopes in two dimensions.

we also express this by saying that **a** majorizes **b**. It is clear that any permutation of **a** also majorizes any permutation of **b**. Note that any vector majorizes itself.

DEFINITION 2. Stochastic Matrices. An $M \times M$ matrix **Q** is said to be **doubly stochastic** if its elements are such that $Q_{ij} \geq 0$, $\sum_j Q_{ij} = 1$, and $\sum_i Q_{ij} = 1$. That is, all elements are nonnegative and the elements in each row (and each column) add to unity. So any row or column can be regarded conceptually as a vector of probabilities. Any permutation matrix **P_i** (i.e., a matrix obtained by a permutation of the columns of the identity matrix) is doubly stochastic. In fact we can generate all doubly stochastic matrices from permutations (see Theorem 3).

DEFINITION 3. Orthostochastic matrices. An $M \times M$ matrix **Q** is said to be orthostochastic if it is constructed from the elements of a unitary matrix **U** of the same size by defining $Q_{ij} = |U_{ij}|^2$. Here is an example:

$$\mathbf{Q} = \begin{bmatrix} \cos^2 \theta & \sin^2 \theta \\ \sin^2 \theta & \cos^2 \theta \end{bmatrix}.$$

Since $\sum_i |U_{ij}|^2 = \sum_j |U_{ij}|^2 = 1$, an orthostochastic matrix is doubly stochastic. Here are some important properties pertaining to these ideas: (1) The **product** of any number of doubly stochastic matrices is doubly stochastic. For the case of two matrices this is readily verified by expressing the elements of the product in terms of the original matrices. By repeated application, the result follows for any number of matrices. (2) Any **convex combination** of doubly stochastic matrices is doubly stochastic. That is, if the **Q_i** are doubly stochastic, then so is $\sum_i \alpha_i \mathbf{Q}_i$ when $\alpha_i \geq 0$, $\sum_i \alpha_i = 1$.

THEOREM 2 (Majorization Theorem). *The real vector **a** majorizes the real vector **b** if and only if there exists a doubly stochastic matrix **Q** such that $\mathbf{b} = \mathbf{Qa}$. The proof can be found in [26, p. 197]; for the case of $M = 2$ the proof is especially simple [69].*

THEOREM 3 (Birkhoff’s Theorem). *An $M \times M$ matrix **Q** is doubly stochastic if and only if it is a convex combination of permutation matrices; that is, it can be expressed as $\mathbf{Q} = \sum_{i=1}^J \alpha_i \mathbf{P}_i$ where $\alpha_i \geq 0$, $\sum_i \alpha_i = 1$, and **P_i** are permutation matrices. For proof see [26, p. 527].*

THEOREM 4 (Orthostochastic Majorization Theorem). *The vector **a** majorizes **b** if and only if there exists an orthostochastic matrix **Q** such that $\mathbf{b} = \mathbf{Qa}$. The “if” part is a consequence of the majorization theorem stated above because orthostochastic matrices are doubly stochastic. For the “only if” part, see [26].*

6. PRINCIPAL COMPONENT FILTER BANKS

In this section we define principal component filter banks formally and prove their optimality for various problems. These results were first presented in [6]. More details can be found in [9]. Unless mentioned otherwise all our discussions are restricted to uniform, maximally decimated filter banks (Fig. 1), which are further assumed to be orthonormal. We often consider a constrained subset or subclass **C** of all such filter banks and talk about a PCFB for this class.

The following examples will clarify the meaning of *classes of filter banks*: (1) The subset of filter banks having only FIR filters of length $\leq M$. So **E(z)** in Fig. 1b is a constant unitary

matrix. This is the class of **transform coders (TC)** denoted as \mathcal{C}^t . (2) The subset of filter banks with no restriction on order (e.g., ideal brickwall filters are allowed). We refer to this as the **unconstrained subband coder (SBC)** class and denote it as \mathcal{C}^u . (3) The subset \mathcal{C}^f of all FIR filter banks with filter lengths \leq some integer N . (4) The subset of cosine modulated filter banks, the subset of DFT filter banks, and so forth [62].

DEFINITION 4. *Principal Component Filter Bank (PCFB).* A filter bank \mathcal{F} in a class \mathcal{C} is said to be a **PCFB** for that class and for the given input psd $\mathbf{S}_{xx}(z)$ if its subband variance vector **majorizes** (Subsection 5.2) all vectors in the set \mathcal{S} of subband variance vectors allowed by the class \mathcal{C} .

The advantage of PCFBs is that they are optimal for several problems as elaborated in Sections 7, 8, 10. The optimality property arises from the result (proved in [9]) that any **concave** function ϕ of the subband variance vector $\mathbf{v} = [\sigma_0^2 \ \sigma_1^2 \ \dots \ \sigma_{M-1}^2]^T$ is *minimized* by a PCFB when one exists. It is possible that PCFBs *do not exist* for certain classes. An example is presented in [31] for a class of FIR filter banks. It is shown in [9] that a PCFB does not in general exist for the class of DFT filter banks or for the class of cosine modulated filter banks [62]. There are some classes for which the PCFB always exists (Section 9).

6.1. Remarks on PCFB Definition

(1) *Uniqueness up to permutation.* If we permute the subbands in a PCFB, the result still remains a PCFB. Moreover, if the variances are ordered according to a convention, say $\sigma_0^2 \geq \sigma_1^2 \geq \sigma_2^2 \geq \dots$, then the PCFB variance vector is unique [69] though the PCFB may not be unique. The PCFB variance vector clearly depends on the input psd $\mathbf{S}_{xx}(z)$ and the class \mathcal{C} of filter banks under consideration.

(2) *A simple optimality property.* Assume again that the variances are ordered according to $\sigma_0^2 \geq \sigma_1^2 \geq \sigma_2^2 \geq \dots$. Suppose the subband processors P_i are multipliers m_i with

$$m_i = \begin{cases} 1 & \text{for } 0 \leq i \leq P \\ 0 & \text{for } P + 1 \leq i \leq M - 1, \end{cases}$$

where P is a fixed integer chosen a priori. This system merely keeps the subbands $0, 1, \dots, P$, and discards the rest (it is a “keep or kill” system). The average error variance in a deleted subband is clearly σ_i^2 . By orthonormality the reconstruction error variance is

$$\frac{1}{M} \sum_{i=P+1}^{M-1} \sigma_i^2 = \sigma_x^2 - \frac{1}{M} \sum_{i=0}^P \sigma_i^2.$$

Since a PCFB by definition has the maximum value for the sum $\sum_{i=0}^P \sigma_i^2$, it follows that the preceding reconstruction error is *minimized* for any choice of P . So the best filter bank to use in the keep or kill system is the PCFB, a well known result [56]. Deeper optimality properties will be presented next.

6.2. PCFB Optimality

The PCFB has deeper optimality properties which make it attractive in many other applications. Let \mathcal{C} be a certain class of (uniform, orthonormal) filter banks and let the input psd matrix $\mathbf{S}_{xx}(z)$ be fixed. Let \mathcal{S} be the set of variance vectors

$$\mathbf{v} = [\sigma_0^2 \ \sigma_1^2 \ \dots \ \sigma_{M-1}^2]^T$$

realizable by this class for this input psd, and let $co(\mathcal{S})$ denote the convex hull of \mathcal{S} .

LEMMA 2 (Polytope Lemma). *If there exists a PCFB for the class \mathcal{C} , then the convex hull $co(\mathcal{S})$ is a convex polytope. Moreover, the extreme points $\{\mathbf{v}_i\}$ of this polytope are permutations of a single vector \mathbf{v}_1 , which is the subband variance vector of the PCFB.*

Since the permutation of filters does not destroy the PCFB property, all the generating vectors $\{\mathbf{v}_i\}$ correspond to PCFBs. The number of distinct permutations of the vector $\mathbf{v}_1 \leq M!$, so the polytope has at most $M!$ extreme points. Next, since the PCFB variance vector is unique upto permutation, the **polytope associated with a PCFB is unique**.

Proof of Lemma 2. Let \mathbf{v}_1 be a variance vector produced by the PCFB. Then \mathbf{v}_1 majorizes all the realizable variance vectors, that is, all vectors in \mathcal{S} . In view of the majorization theorem (Subsection 5.2) any vector $\mathbf{v} \in \mathcal{S}$ can therefore be written as $\mathbf{v} = \mathbf{Q}\mathbf{v}_1$ where \mathbf{Q} is a doubly stochastic matrix. Next, using Birkhoff's theorem (Subsection 5.2) we can express \mathbf{Q} as a convex combination of permutation matrices \mathbf{P}_i , that is, $\mathbf{Q} = \sum_i \alpha_i \mathbf{P}_i$ where $\alpha_i \geq 0$ and $\sum \alpha_i = 1$. Thus $\mathbf{v} = \mathbf{Q}\mathbf{v}_1 = \sum_{i=1}^J \alpha_i \mathbf{P}_i \mathbf{v}_1 = \sum_{i=1}^J \alpha_i \mathbf{v}_i$ where the \mathbf{v}_i are permutations of \mathbf{v}_1 . Thus any vector \mathbf{v} in \mathcal{S} is a convex combination of permutations of the PCFB variance vector \mathbf{v}_1 . That is, $\mathcal{S} \subset co\{\mathbf{v}_i\}$, where $co\{\mathbf{v}_i\}$ denotes the convex polytope generated by $\{\mathbf{v}_i\}$. By definition \mathbf{v}_1 is in \mathcal{S} and so are all the permutations \mathbf{v}_i . This shows that $co\{\mathbf{v}_i\} \subset co(\mathcal{S})$. In short $\mathcal{S} \subset co\{\mathbf{v}_i\} \subset co(\mathcal{S})$. Since $co(\mathcal{S})$ is the smallest convex set containing \mathcal{S} and $co\{\mathbf{v}_i\}$ is convex, it is obvious that $co\{\mathbf{v}_i\} = co(\mathcal{S})$. Summarizing, the convex hull $co(\mathcal{S})$ is the polytope $co\{\mathbf{v}_i\}$ generated by $\{\mathbf{v}_i\}$. ■

THEOREM 5 (Optimality of PCFB). *Assume the input psd $\mathbf{S}_{xx}(z)$ and the filter bank class \mathcal{C} fixed, so that the set \mathcal{S} of realizable variance vectors is fixed. Let $g(\mathbf{v})$ be a concave function with domain given by the convex set $co(\mathcal{S})$. Assume the PCFB exists so that $co(\mathcal{S})$ is the convex polytope generated by the PCFB variance vectors $\{\mathbf{v}_i\}$ (Lemma 2). Then there exists a PCFB variance vector, say \mathbf{v}_1 , such that*

$$g(\mathbf{v}_1) \leq g(\mathbf{v})$$

for any $\mathbf{v} \in co(\mathcal{S})$. This means in particular that $g(\mathbf{v}_1) \leq g(\mathbf{v})$ for any $\mathbf{v} \in \mathcal{S}$, that is, \mathbf{v}_1 is at least as good as any other realizable variance vector \mathbf{v} . Summarizing, the concave function $g(\mathbf{v})$ is minimized at one of the extreme points of the convex polytope $co(\mathcal{S})$, i.e., by one of the PCFBs.

Proof. Let \mathbf{v}_1 be a vector in the finite set $\{\mathbf{v}_i\}$ such that $g(\mathbf{v}_1) \leq g(\mathbf{v}_i)$ for all i . Since $co(\mathcal{S})$ is a convex polytope generated by $\{\mathbf{v}_i\}$, any vector $\mathbf{v} \in co(\mathcal{S})$ has the form

$\mathbf{v} = \sum_{i=1}^J \alpha_i \mathbf{v}_i$ where $\alpha_i \geq 0$ and $\sum_i \alpha_i = 1$. We now have

$$g(\mathbf{v}) = g\left(\sum_{i=1}^J \alpha_i \mathbf{v}_i\right) \geq \sum_{i=1}^J \alpha_i g(\mathbf{v}_i) \geq \sum_{i=1}^J \alpha_i g(\mathbf{v}_1) = g(\mathbf{v}_1),$$

where the first inequality follows from concavity. So we have proved $g(\mathbf{v}_1) \leq g(\mathbf{v})$ indeed. ■

6.3. More on PCFB and Convex Polytopes

We now prove a few more results pertaining to the connection between polytopes and PCFBs.

LEMMA 3. *Let \mathcal{S} be the set of variance vectors associated with a class of orthonormal filter banks \mathcal{C} . Suppose the convex hull $co(\mathcal{S})$ is a polytope generated by a minimal set of vectors $\{\mathbf{v}_1, \mathbf{v}_2, \dots, \mathbf{v}_J\}$. Then $\mathbf{v}_k \in \mathcal{S}$, that is, each \mathbf{v}_k is a realizable variance vector.*

Proof. Since the vectors \mathbf{v}_k are in $co(\mathcal{S})$, they are convex combinations of vectors in \mathcal{S} . And since \mathbf{v}_k are extreme points of $co(\mathcal{S})$ (Lemma 1) they can only be trivial convex combinations of members of $co(\mathcal{S})$. Combining these we conclude that $\mathbf{v}_k = \mathbf{s}_k$ for some $\mathbf{s}_k \in \mathcal{S}$. In short, $\mathbf{v}_k \in \mathcal{S}$. ■

LEMMA 4 (Converse of the Polytope Lemma). *Let \mathcal{S} be the set of variance vectors associated with a class \mathcal{C} of orthonormal filter banks. Suppose the convex hull $co(\mathcal{S})$ is a polytope generated by a minimal set of vectors $\{\mathbf{v}_1, \mathbf{v}_2, \dots, \mathbf{v}_J\}$ and furthermore, all these \mathbf{v}_k are permutations of \mathbf{v}_1 . Then the \mathbf{v}_k are not only realizable as shown above but in addition the filter banks which realize \mathbf{v}_k are PCFBs for the class \mathcal{C} .*

Proof. Let \mathbf{v} be any realizable variance vector. Since $\mathbf{v} \in \mathcal{S}$, it is a convex combination of $\{\mathbf{v}_k\}$. So $\mathbf{v} = \sum_k \alpha_k \mathbf{v}_k = \sum_k \alpha_k \mathbf{P}_k \mathbf{v}_1 = \mathbf{Q} \mathbf{v}_1$ where \mathbf{P}_k are permutation matrices. The matrix \mathbf{Q} is doubly stochastic because it is a convex combination of permutations (Birkhoff's theorem, Subsection 5.2). This shows that \mathbf{v}_1 majorizes \mathbf{v} (majorization theorem, Subsection 5.2). The filter bank realizing \mathbf{v}_1 is therefore a PCFB and so are filter banks realizing any of the variance vectors \mathbf{v}_k . ■

THEOREM 6 (PCFBs and Convex Polytopes). *The polytope lemma and its converse can be combined to obtain the following result: There exists a PCFB for a class of filter banks \mathcal{C} for a given input psd $\mathbf{S}_{xx}(z)$ if and only if the convex hull $co(\mathcal{S})$ of the set \mathcal{S} of realizable subband variances is a convex polytope generated by permutations of a single variance vector \mathbf{v}_1 . This variance vector is itself realizable by the PCFB.*

7. REVISITING WELL KNOWN OPTIMIZATION PROBLEMS

In Section 2 we stated some well known filter bank optimization problems. In the majority of these examples the subband processors are quantizers and the reconstruction error of the filter bank is given by

$$\sigma_e^2 = \sum_i f_i(b_i) \sigma_i^2 / M,$$

where $f_i(b_i)$ are normalized distortion rate functions of the quantizers. Assume that the functions $f_i(\cdot)$ are **independent** of the filter bank. Since $f_i(b_i)\sigma_i^2$ is concave in σ_i^2 it follows that σ_e^2 is a concave function of the variance vector $[\sigma_0^2 \ \sigma_1^2 \ \dots \ \sigma_{M-1}^2]^T$. If we are searching for a (uniform orthonormal) filter bank in a certain class \mathcal{C} to minimize σ_e^2 then the best solution is indeed a PCFB in \mathcal{C} (from Theorem 5). A different proof of this was presented in [32]. Since all permutations of a PCFB are still PCFBs, we can perform a finite search and compute the quantity σ_e^2 for each of the PCFBs and choose the best.⁷

Note that this proves optimality of the PCFB regardless of the exact detail of the quantizer functions $f_i(b_i)$. They need not be high bit-rate functions of the form $f_i(b_i) = c_i 2^{-2b_i}$, and the bit-allocation need not be optimal. In fact $f_i(b_i)$ can just take binary values of 0 and 1 (the keep-or-kill system), in which case the reconstructed signal is then a *partial reconstruction* from a subset of subbands.

Remarks on ordering of the filters. Since any permutation of a PCFB is still a PCFB it remains to figure out the correct permutation that minimizes σ_e^2 . This depends on the relative values of the normalized quantizer functions $f_i(b_i)$. Now consider a sum of two terms $A\sigma_i^2 + B\sigma_j^2$ and assume $A \leq B$. If $\sigma_i^2 < \sigma_j^2$ then we can obtain a smaller sum $A\sigma_j^2 + B\sigma_i^2$ by interchanging the variances σ_i^2 and σ_j^2 . So, assuming the ordering convention $f_i(b_i) \leq f_{i+1}(b_{i+1})$ we see that the correct permutation to choose for the PCFB should be such that

$$\sigma_0^2 \geq \sigma_1^2 \geq \dots \geq \sigma_{M-1}^2.$$

For example, suppose all the quantizer functions are identical and equal to $f(b_j)$ (i.e., use the same kind of quantizer in all subbands). Assuming that $f(b_j)$ decreases as b_j increases we see that if $b_0 \geq b_1 \geq \dots$, then the PCFB with $\sigma_0^2 \geq \sigma_1^2 \geq \dots$ should be used (use more bits for subband with higher variance).

8. OPTIMAL NOISE REDUCTION WITH FILTER BANKS

Return to the orthonormal filter bank and assume that the input $x(n)$ is a real noisy signal $x(n) = s(n) + \mu(n)$ where $s(n)$ is the signal component and $\mu(n)$ is noise (Fig. 11). Assume that the subband processors are constant real multipliers m_i to be chosen such that $\hat{x}(n)$ represents $s(n)$ better than $x(n)$ does.

Suppose we wish to choose the analysis filters and the multipliers m_i such that the error $\hat{x}(n) - s(n)$ is minimized in the mean square sense. We assume: (1) $s(n)$ and $\mu(n)$ are jointly WSS and have zero mean, (2) the noise $\mu(n)$ is white with variance η^2 , and (3) $\mu(n)$ is uncorrelated to $s(n)$. Then the subband signals $y_k(n)$ have the form $y_k(n) = s_k(n) + \mu_k(n)$ where the signal part $s_k(n)$ and noise part $\mu_k(n)$ are uncorrelated with zero mean. By orthonormality of the filter bank, each $\mu_k(n)$ is white with variance η^2 . Let σ_k^2 denote the variance of the signal part $s_k(n)$. We consider two schemes for choice of the multipliers.

Scheme 1. Wiener filters. The value of m_k will be chosen such that the error $q_k(n) \triangleq m_k y_k(n) - s_k(n)$ is minimized in the mean square sense. The best m_k is the **Wiener**

⁷ In fact $f_i(b_i)\sigma_i^2$ is linear in σ_i^2 which means that it is concave as well as convex. This means that the PCFB minimizes the objective for certain choice of ordering of the filters and maximizes the same objective for some permuted ordering.

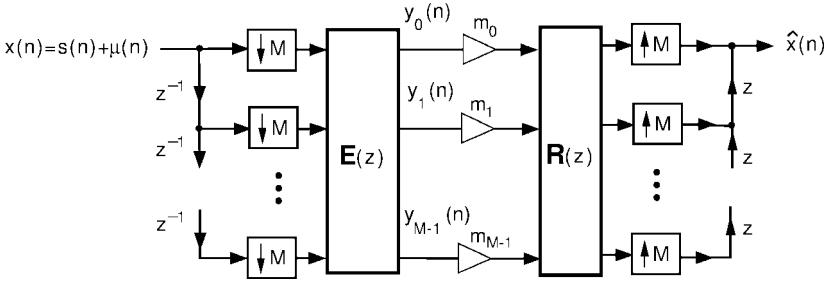


FIG. 11. The M -channel maximally decimated filter bank with noisy input. The subband processors are constant multipliers which seek to improve the signal-to-noise ratio.

solution, namely, $m_k = \sigma_k^2 / (\sigma_k^2 + \eta^2)$. Then the subband error component $m_k y_k(n) - s_k(n)$ has the variance $\sigma_{q_k}^2 = \eta^2 \sigma_k^2 / (\eta^2 + \sigma_k^2)$. For fixed η^2 this function is plotted in Fig. 12a and is **concave** with respect to σ_k^2 . The error in the reconstructed signal $\hat{x}(n) - s(n)$ has variance

$$\frac{1}{M} \sum_k \sigma_{q_k}^2 = \frac{1}{M} \sum_{k=0}^{M-1} \frac{\eta^2 \sigma_k^2}{\eta^2 + \sigma_k^2}.$$

Since the k th term is concave in σ_k^2 , this quantity is a concave function of the subband variance vector $[\sigma_0^2 \ \sigma_1^2 \ \dots \ \sigma_{M-1}^2]^T$. It follows from Theorem 5 that this quantity is **minimized** if the filter bank is chosen to be a **PCFB** for the input signal component $s(n)$, with appropriate ordering of subbands.

Scheme 2. Hard threshold devices. A hard threshold operator in the subband [18] can be represented by a multiplier of the form

$$m_k = \begin{cases} 0 & \text{if } \sigma_k^2 < \eta^2 \\ 1 & \text{if } \sigma_k^2 \geq \eta^2 \end{cases} \quad (9)$$

which is demonstrated in Fig. 12b. Then the error signal $q_k(n) \triangleq m_k y_k(n) - s_k(n)$ is given by

$$q_k(n) = \begin{cases} -s_k(n) & \text{if } \sigma_k^2 < \eta^2 \\ \mu_k(n) & \text{if } \sigma_k^2 \geq \eta^2. \end{cases}$$

Its variance $\sigma_{q_k}^2$ is therefore as shown in Fig. 12c. This again is a concave function of σ_k^2 . The error in the reconstructed signal $\hat{x}(n) - s(n)$ has variance $(1/M) \sum_k \sigma_{q_k}^2$ and is therefore concave in the signal variance vector. This is minimized if the filter bank is a PCFB for $s(n)$, with appropriate ordering of subbands.

Notice that the PCFB optimality holds even with m_k chosen according to scheme 1 in some subbands and scheme 2 in others. These results do not hold if $\mu(n)$ is **colored noise**, for in that case, the noise variances η_k^2 in the subbands depend on the choice of analysis filters and cannot be regarded as constants. Notice finally that if the threshold value T in hard-thresholding is chosen to be different from η^2 then the concavity property is lost [69], and PCFB optimality is not established.

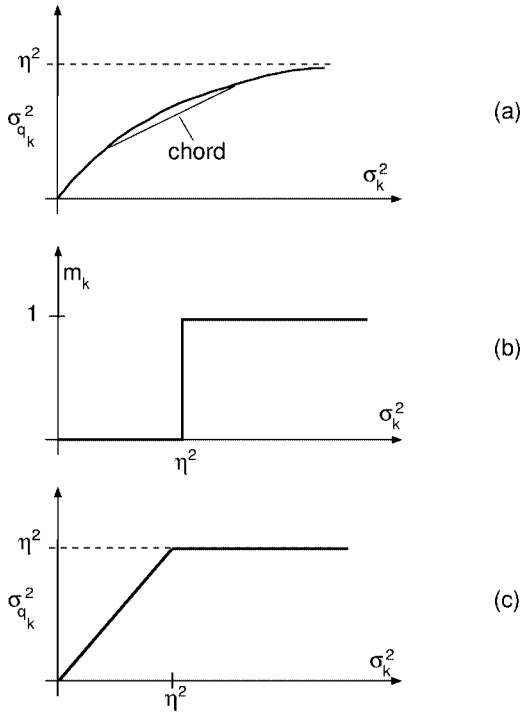


FIG. 12. (a) The variance of subband reconstruction error when a subband Wiener filter is used, (b) hard thresholding nonlinearity, and (c) the variance of subband reconstruction error when hard thresholding is used.

9. STANDARD FILTER BANK CLASSES WITH PCFB

In this section we consider a number of filter bank classes which have a PCFB. In each case we also relate the PCFB to the geometric insight obtained from Theorem 6 on convex polytopes.

9.1. Two-Channel Case

First consider the **two-channel** orthonormal filter bank ($M = 2$). Owing to orthonormality of the filter bank, the subband variances σ_i^2 are related to input variance σ_x^2 by $\sigma_0^2 + \sigma_1^2 = 2\sigma_x^2$.

The PCFB by definition is the filter bank with the property that σ_0^2 is maximized within the class \mathcal{C} . We therefore optimize the filters in the specified class \mathcal{C} such that one subband has maximum variance κ^2 (i.e., the filter $H_0(z)$ is an optimum compaction filter). So a **PCFB exists** regardless of any further constraints that might be imposed on $H_0(z)$ such as the rational or FIR constraint. The solutions for various choices of the class \mathcal{C} such as the FIR class, stable IIR class, and infinite order (ideal filter) class have been discussed in various papers [33, 57, 60, 66]. From Theorem 6 we know that the set of realizable subband variance vectors has a convex hull which is a convex polytope. The extreme points of this polytope are the variance vectors $[\kappa^2 \quad 2\sigma_x^2 - \kappa^2]^T$ and its permutation $[2\sigma_x^2 - \kappa^2 \quad \kappa^2]^T$. The convex polytope is therefore the **straightline segment** shown in Fig. 13, with the exact value of κ^2 depending on the class \mathcal{C} and the input psd.

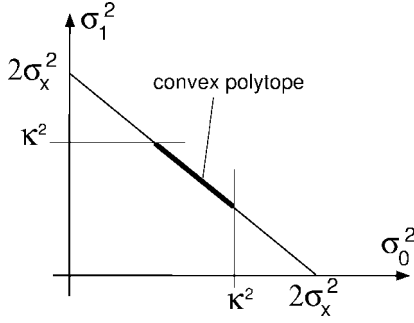


FIG. 13. The convex hull (polytope) of allowed subband variance vectors for the two-channel case.

9.2. Arbitrary Number of Channels, Transform Coder Class

For the transform coder class \mathcal{C}^t , $\mathbf{E}(z)$ of Fig. 1b is a constant unitary matrix \mathbf{T} , and the filters $H_k(z)$ have length $\leq M$. If \mathbf{T} is the KLT, the decimated subband signals $y_k(n)$ and $y_m(n)$ ($m \neq k$) are uncorrelated for each n . Let $\mathbf{R}_{xx} = E[\mathbf{x}(n)\mathbf{x}^\dagger(n)]$ be the autocorrelation matrix of $\mathbf{x}(n)$ in Fig. 1b, with eigenvalues λ_i . Then we have the following:

THEOREM 7 (KLT, PCFB, and Convex Polytopes). *For the transform coder class \mathcal{C}^t :*
 (a) *The KLT is a PCFB.* (b) *The set \mathcal{S} of realizable variances for the class \mathcal{C}^t is the set of all variance vectors of the form $\mathbf{b} = \mathbf{Q}\mathbf{a}$ where \mathbf{Q} is orthostochastic, and \mathbf{a} the KLT subband-variance vector:*

$$\mathbf{a} = [\lambda_0 \lambda_1 \dots \lambda_{M-1}]^T.$$

(c) *Equivalently \mathcal{S} is the set of all variance vectors majorized by \mathbf{a} .* (d) *Finally \mathcal{S} is itself a convex polytope generated by permutations of \mathbf{a} . This clearly means that \mathcal{S} is its own convex hull, i.e., $\text{co}(\mathcal{S}) = \mathcal{S}$.*

Proof. Part (a) is well known, but here is a proof for completeness, based on the orthostochastic majorization Theorem 4. A more self contained proof can be found in [45]. Let $\mathbf{w}(n)$ denote the decimated subband vector for arbitrary unitary \mathbf{T} and $\mathbf{y}(n)$ the subband vector when \mathbf{T} is chosen as the KLT. Then $\mathbf{w}(n) = \mathbf{U}\mathbf{y}(n)$ for some unitary \mathbf{U} . So $\mathbf{R}_{ww} = \mathbf{U}\mathbf{A}\mathbf{U}^\dagger$ where $\mathbf{R}_{ww} = E[\mathbf{w}(n)\mathbf{w}^\dagger(n)]$, and $\mathbf{A} = E[\mathbf{y}(n)\mathbf{y}^\dagger(n)]$ is the diagonal matrix of the eigenvalues λ_i . Since $[\mathbf{R}_{ww}]_{ii}$ are the variances σ_i^2 of elements of $\mathbf{w}(n)$,

$$\sigma_i^2 = \sum_{n=0}^{M-1} \lambda_n |\mathbf{U}_{in}|^2. \quad (10)$$

The variance vector $\mathbf{b} = [\sigma_0^2 \sigma_1^2 \dots \sigma_{M-1}^2]^T$ is therefore given by $\mathbf{b} = \mathbf{Q}\mathbf{a}$ where \mathbf{Q} has the elements $|\mathbf{U}_{in}|^2$. Thus \mathbf{Q} is orthostochastic, and Theorem 4 shows that \mathbf{a} majorizes \mathbf{b} . This proves that KLT is a PCFB solution.

We just showed that any realizable variance vector has the form $\mathbf{b} = \mathbf{Q}\mathbf{a}$. For part (b) we have to show the converse of this. Consider any vector of the form $\mathbf{b} = \mathbf{Q}\mathbf{a}$ where \mathbf{Q} is some orthostochastic matrix. By definition of orthostochastic property, there is a unitary \mathbf{U} such that $[\mathbf{Q}]_{in} = |\mathbf{U}_{in}|^2$. If we cascade the matrix \mathbf{U} after the KLT matrix \mathbf{T} , the subband coder output will have the variance vector \mathbf{b} . So any vector of the form $\mathbf{b} = \mathbf{Q}\mathbf{a}$

is a valid variance vector for the class \mathcal{C}^t , proving part (b). Part (c) follows then from the orthostochastic majorization theorem (Subsection 5.2). Finally consider part (d). We showed that any member of \mathcal{S} has the form \mathbf{Qa} for some orthostochastic \mathbf{Q} . Vectors in \mathcal{S} are therefore convex combinations of permutations of \mathbf{a} (from Birkhoff’s theorem, Subsection 5.2). Conversely, let \mathbf{c} be any convex combination of permutations of \mathbf{a} . Using Birkhoff’s theorem we can write $\mathbf{c} = \mathbf{Pa}$ for some doubly stochastic \mathbf{P} . This shows that \mathbf{a} majorizes \mathbf{c} . By Theorem 4 there is an orthostochastic \mathbf{Q} such that $\mathbf{c} = \mathbf{Qa}$. In view of part (b) this implies that \mathbf{c} is in \mathcal{S} . Thus any convex combination of permutations of \mathbf{a} is in \mathcal{S} . ■

9.3. Arbitrary Number of Channels, Unconstrained Subband Coder Class

Consider the unconstrained class \mathcal{C}^u of orthonormal filter banks with unrestricted filter order. For this class a PCFB exists [56, 66]. To see this let $\mathbf{S}_{xx}(e^{j\omega})$ be the psd matrix of the vector process $\mathbf{x}(n)$. Denote the psd of $y_k(n)$ as $S_k(e^{j\omega})$. Suppose we choose $\mathbf{E}(e^{j\omega})$ to be the KLT for $\mathbf{S}_{xx}(e^{j\omega})$, pointwise for each ω . Then the output psd matrix $\mathbf{S}_{yy}(e^{j\omega})$ is diagonal with elements $S_k(e^{j\omega})$ on the diagonal. Using the argument given in proving part (a) of Theorem 7, we see that the subband psd vector

$$\mathbf{s}(e^{j\omega}) = [S_0(e^{j\omega}) \ S_1(e^{j\omega}) \ \dots \ S_{M-1}(e^{j\omega})]^T \tag{11}$$

majorizes all other subband psd vectors in \mathcal{C}^u . For each ω let the rows of $\mathbf{E}(e^{j\omega})$ be ordered such that

$$S_0(e^{j\omega}) \geq S_1(e^{j\omega}) \geq \dots \geq S_{M-1}(e^{j\omega}). \tag{12}$$

Since the subband variances are $\sigma_i^2 = \int_0^{2\pi} S_i(e^{j\omega}) d\omega/2\pi$, it then follows that the subband variance vector majorizes all other subband variance vectors allowed by the class \mathcal{C}^u . The ordering (12) has been referred to as spectral majorization [66] (see Subsection 3.2). Thus the pointwise KLT property together with spectral majorization yields the PCFB property. The pointwise KLT property ensures that the decimated subbands processes are uncorrelated, i.e., $E[y_k(n)y_i^*(m)] = 0$ for $k \neq i$ for any pair m, n . This is the total decorrelation property, evidently stronger than the instantaneous decorrelation property of traditional KLT (i.e., $E[y_k(n)y_i^*(n)] = 0$ for each n). In Subsection 3.2 we showed that total decorrelation and spectral majorization are together necessary and sufficient for maximizing the AM/GM ratio (4) of an orthonormal filter bank in the class \mathcal{C}^u . This is another way to see that the PCFB maximizes this ratio.⁸

THEOREM 8. *For the unconstrained filter bank class \mathcal{C}^u , the set \mathcal{S} of realizable variance vectors is itself convex (i.e., $\mathcal{S} = co(\mathcal{S})$). More precisely, \mathcal{S} is the convex polytope generated by the permutations of the PCFB variance vector.*

Proof. Let \mathbf{a} be the PCFB subband variance vector. Any subband variance vector \mathbf{b} for class \mathcal{C}^u is majorized by \mathbf{a} , so we have $\mathbf{b} = \mathbf{Qa}$ for some orthostochastic \mathbf{Q} (Theorem 4). Conversely given any vector of the form $\mathbf{b} = \mathbf{Qa}$, let \mathbf{T} be a unitary matrix associated with the orthostochastic \mathbf{Q} . If we insert \mathbf{T} after the PCFB $\mathbf{E}(e^{j\omega})$ in Fig. 1b the subband

⁸The AM/GM ratio has the interpretation of coding gain under certain conditions as explained in Subsection 3.2.

variance vector will be \mathbf{b} , showing that \mathbf{b} is realizable. Summarizing, the set \mathcal{S} of all realizable subband vectors for class \mathcal{C}^u is the set of all vectors of the form $\mathbf{b} = \mathbf{Q}\mathbf{a}$ where \mathbf{Q} is orthostochastic and \mathbf{a} is the fixed PCFB vector. So the set \mathcal{S} is the convex polytope generated by permutations of \mathbf{a} . ■

Remark. The preceding argument holds for classes broader than \mathcal{C}^l and \mathcal{C}^u and fails only when constant unitary matrices cannot be inserted without violating the class constraint (e.g., DFT or cosine modulated filter banks). Thus *as long as the class has a PCFB and allows us to insert constant unitary matrices arbitrarily*, the set of realizable variances is the convex polytope generated by permutations of the PCFB variance vector.

10. THE DISCRETE MULTITONE (DMT) COMMUNICATION SYSTEM

In Fig. 1 we saw the traditional maximally decimated analysis/synthesis system used in subband coding. A dual of this system, called the **transmultiplexer** circuit, is commonly used for conversion between time domain and frequency domain multiplexing [62, 70]. More recently this system has found application in the digital implementation of multicarrier systems, more popularly known as the **DMT** (discrete multitone) modulation systems (Fig. 14). Here $C(z)$ represents the transfer function of a linear channel with additive noise $e(n)$. In Subsection 1.2 we defined the filter bank of Fig. 1 to be biorthogonal if the condition $H_k(e^{j\omega})F_m(e^{j\omega})|_{\downarrow M} = \delta(k - m)$ is satisfied. Under this condition $\hat{x}(n) = x(n)$ for all n in Fig. 1 (in absence of subband processing). It can be shown that the same biorthogonality implies

$$y_k(n) = x_k(n)$$

for all k, n in Fig. 14, assuming a perfect channel ($C(z) = 1$ and $e(n) = 0$). As in Subsection 1.2 the filters $\{F_k(z)\}$ are said to be **orthonormal** if $F_k(e^{j\omega})F_m^*(e^{j\omega})|_{\downarrow M} = \delta(k - m)$ (equivalently the polyphase matrix $\mathbf{R}(z)$ is paraunitary). In this case biorthogonality or perfect reconstruction is achieved by choosing $H_k(e^{j\omega}) = F_k^*(e^{j\omega})$. The use of filter bank theory in the optimization of DMT systems has been of some interest in the past [37, 38]. We have shown recently [68] that the principal component filter bank, which is known to be optimal for several problems involving the subband coder, will also be optimal in many respects for the DMT communications system.

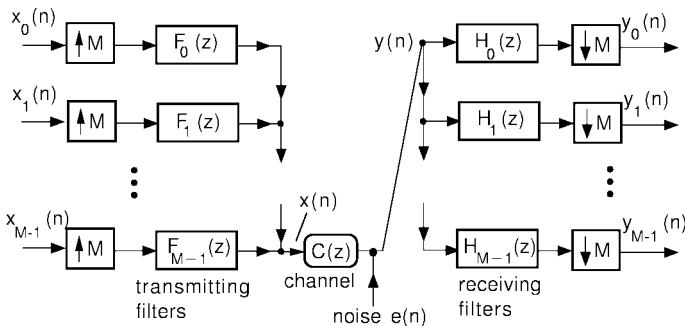


FIG. 14. The discrete multitone communication system.

Figure 14 shows only the essentials of discrete multitone communication. Background material on the DMT system and more generally on the use of digital filter banks in communications can be found in [3, 13, 29, 30, 59]. Excellent tutorial presentations can be found in [12]. Briefly, here is how the system works: the signals $x_k(n)$ are b_k -bit symbols obtained from a PAM or QAM constellation (see Appendix B). Together these signals represent $\sum_k b_k = b$ bits and are obtained from a b -bit block of a binary data stream (Appendix B). The symbols $x_k(n)$ are then interpolated M -fold by the filters $F_k(z)$. Typically the filters $\{F_k(e^{j\omega})\}$ constitute an orthonormal filter bank and their passbands cover different uniform regions of digital frequency $0 \leq \omega \leq 2\pi$. The outputs of $F_k(z)$ can be regarded as modulated versions of the symbols. These are packed into M adjacent frequency bands (passbands of the filters) and added to obtain the composite signal $x(n)$. This is then sent through the channel which is represented by a transfer function $C(z)$ and additive Gaussian noise $e(n)$ with power spectrum $S_{ee}(e^{j\omega})$. In actual practice the channel is a continuous-time system preceded by D/A conversion and followed by A/D conversion. We have replaced this with discrete equivalents $C(z)$ and $e(n)$.

The received signal $y(n)$ is a distorted and noisy version of $x(n)$. The receiving filter bank $\{H_k(z)\}$ separates this signal into the components $y_k(n)$ which are distorted and noisy versions of the symbols $x_k(n)$. The task at this point is to correctly detect the value of $x_k(n)$ from $y_k(n)$. There is a probability of error in this detection which depends on the signal and noise levels.

If the filter bank $\{F_k, H_m\}$ is biorthogonal then we have the perfect reconstruction property $y_k(n) = x_k(n)$ in absence of channel imperfections (i.e., assuming $C(z) = 1$ and $e(n) = 0$). In practice we cannot assume this. We will assume that $\{F_k, H_m\}$ is biorthogonal (in fact orthonormal, see below) and that the receiving filters are $H_k(z)/C(z)$ instead of $H_k(z)$, so that $C(z)$ is compensated or **equalized** completely.

10.1. Probability of Error

For simplicity we assume that $x_k(n)$ are PAM symbols (Appendix B). Assuming that $x_k(n)$ is a random variable with 2^{b_k} equiprobable levels, its variance represents the **average power** P_k in the symbol $x_k(n)$. The Gaussian channel noise $e(n)$ is filtered through $H_k(z)/C(z)$ and decimated by M . For the purpose of variance calculation, the model for the noise $q_k(n)$ at the detector input can therefore be taken as in Fig. 15. Let $\sigma_{q_k}^2$ be the variance of $q_k(n)$. Then the **probability of error** in detecting the symbol $x_k(n)$ can be expressed in closed form [49] and is given by

$$\mathcal{P}_e(k) = 2(1 - 2^{-b_k})\mathcal{Q}\left(\sqrt{\frac{3P_k}{(2^{2b_k} - 1)\sigma_{q_k}^2}}\right), \quad (13)$$

where $\mathcal{Q}(v) \triangleq \int_v^\infty e^{-u^2/2} du / \sqrt{2\pi}$ (area of the normalized Gaussian tail).

10.2. Minimizing Transmitted Power

Since the \mathcal{Q} -function can be inverted for any nonnegative argument, we can invert (13) to obtain

$$P_k = \beta(\mathcal{P}_e(k), b_k) \times \sigma_{q_k}^2, \quad (14)$$

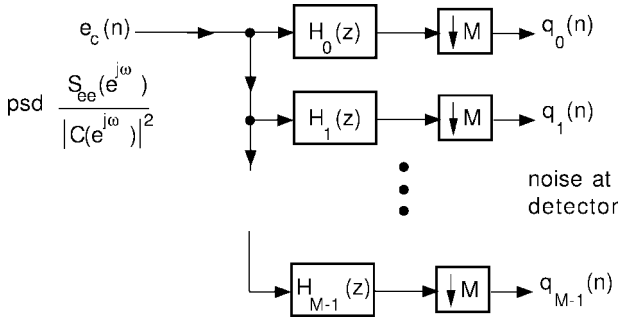


FIG. 15. A model for noise at the detector input.

where the exact nature of the function $\beta(\cdot, \cdot)$ is not of immediate interest. This expression says that if the probability of error has to be $\mathcal{P}_e(k)$ or less at the bit rate b_k , then the power in $x_k(n)$ has to be at least as large as P_k . The total transmitted power is therefore

$$P = \sum_{k=0}^{M-1} P_k = \sum_{k=0}^{M-1} \beta(\mathcal{P}_e(k), b_k) \times \sigma_{q_k}^2. \quad (15)$$

Let us assume that the bit rates b_k and probabilities of error $\mathcal{P}_e(k)$ are fixed. For this desired combination of $\{b_k\}$ and $\{\mathcal{P}_e(k)\}$, the total power required depends on the distribution of noise variances $\{\sigma_{q_k}^2\}$.

From Eq. (14) we see that the power P_k in the k th band is a linear (hence concave) function⁹ of $\sigma_{q_k}^2$. The total transmitted power P is therefore a concave function of the noise variance vector

$$[\sigma_{q_0}^2 \ \sigma_{q_1}^2 \ \dots \ \sigma_{q_{M-1}}^2]^T. \quad (16)$$

From Fig. 15 we see that this is the vector of subband variances for the orthonormal filter bank $\{H_k(e^{j\omega})\}$ in response to the power spectrum $S_{ee}(e^{j\omega})/|C(e^{j\omega})|^2$. Recalling the discussion on PCFBs from Subsection 6.2 we now see that the orthonormal filter bank $\{H_k(e^{j\omega})\}$ which **minimizes total power** for fixed error probabilities and bit rates is indeed a **PCFB** for the power spectrum

$$S_{ee}(e^{j\omega})/|C(e^{j\omega})|^2.$$

Having identified this PCFB, the variances $\sigma_{q_k}^2$ are readily computed, from which the powers P_k for fixed bit rate b_k and error probability $\mathcal{P}_e(k)$ can be found (using (14)), and the minimized power P calculated.

10.3. Maximizing Total Bit Rate

Returning to the error probability expression (13) let us now invert it to obtain a formula for the bit rate b_k . This is tricky because of the way b_k occurs in two places. The factor

⁹ A linear function is also convex, so there is a permutation of the optimal PCFB which maximizes rather than minimizes power. Evidently it should be avoided!

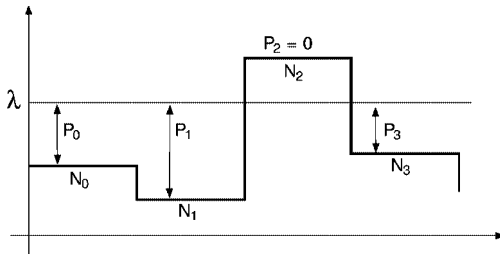


FIG. 16. Optimal power allocation by water pouring.

$(1 - 2^{-b_k})$ however is a weak function of b_k in the sense that it varies from 0.5 to 1 as b_k changes from one to infinity. So we will replace $(1 - 2^{-b_k})$ with unity. Then Eq. (13) yields

$$b_k = 0.5 \log_2 \left(1 + \frac{3}{[Q^{-1}(\mathcal{P}_e(k)/2)]^2} \frac{P_k}{\sigma_{qk}^2} \right)$$

so the total bit rate is

$$b = 0.5 \sum_{k=0}^{M-1} \log_2 \left(1 + \frac{3}{[Q^{-1}(\mathcal{P}_e(k)/2)]^2} \frac{P_k}{\sigma_{qk}^2} \right). \tag{17}$$

This is the bit rate achieved by the DMT system without channel coding, for fixed error probabilities $\{\mathcal{P}_e(k)\}$ and powers $\{P_k\}$. Since function $\log_2(1 + a/x)$ is convex in x (for $a, x > 0$), the total bit rate is convex in the variance vector (16). Thus the orthonormal filter bank $\{H_k(e^{j\omega})\}$ which maximizes bit rate for fixed error probabilities and powers is again a PCFB for the same power spectrum $S_{ee}(e^{j\omega})/|C(e^{j\omega})|^2$ as before. This is very appealing since the maximization of bit rate and minimization of total power are consistent goals.

The preceding result is true regardless of how the total power $P = \sum_k P_k$ is allocated among the bands. In particular we can perform **optimum power allocation**. We have

$$b = 0.5 \sum_{k=0}^{M-1} \log_2 \left(1 + \frac{P_k}{N_k} \right),$$

where $N_k = \sigma_{qk}^2 [Q^{-1}(\mathcal{P}_e(k)/2)]^2/3$. The optimization of $\{P_k\}$ for fixed total power $P = \sum_k P_k$ is a standard problem in information theory [14]. The solution is given by

$$P_k = \begin{cases} \lambda - N_k & \text{if this is nonnegative,} \\ 0 & \text{otherwise,} \end{cases} \tag{18}$$

where λ is chosen to meet the power constraint. This is demonstrated in Fig. 16 and is called the **water pouring** rule.¹⁰ This power allocation is optimal regardless of the exact choice of the filter bank $\{H_k(z)\}$. In particular if $\{H_k(z)\}$ is chosen as the optimal PCFB

¹⁰ Imagine a vessel whose bottom is not flat, but described by the levels N_0, N_1 , and so forth. If this is filled with an amount of water equal to P then this amount divides itself into P_0, P_1 , and so forth automatically.

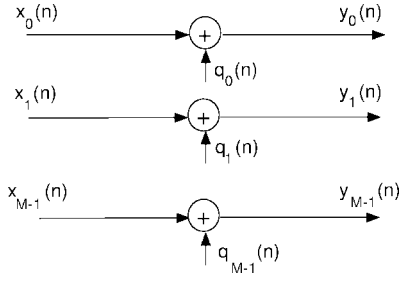


FIG. 17. Equivalent DMT system for noise analysis.

and then power is allocated as above, it provides the maximum possible DMT bit rate b for fixed total power and fixed set of error probabilities.

10.4. Capacity

We conclude by observing some similarities and differences between the actual bit rate (17) and the theoretical capacity of the DMT system. The biorthogonal DMT system with ideal channel equalizer can be represented by the model shown in Fig. 17 where $x_k(n)$ are the modulation symbols and $q_k(n)$ the noise components shown in Fig. 15. In general it is not true that the effective noise components $q_k(n)$ are Gaussian, white, and uncorrelated. However, if the number of bands M is large and the filters $H_k(z)$ are good approximations to ideal filters then this is nearly the case. In this case the channel shown in Fig. 17 is identical to the parallel Gaussian channel and has capacity [14]

$$\mathcal{C} = 0.5 \sum_{k=0}^{M-1} \log_2 \left(1 + \frac{P_k}{\sigma_{q_k}^2} \right). \quad (19)$$

Since the noise variances $\sigma_{q_k}^2$ depend on the filters $\{F_k, H_k\}$, the above capacity \mathcal{C} also depends on them. For the case where $\{F_k\}$ is an orthonormal filter bank this **capacity is maximized** if $\{F_k\}$ is chosen as a PCFB for the power spectrum $S_{ee}(e^{j\omega})/|C(e^{j\omega})|^2$. The reason again is that (19) is convex in the variance vector (16). Moreover, as in [14], we can optimally allocate the powers P_k under a power constraint $P = \sum_k P_k$.

Equation (17) is the **bit rate achieved** for fixed probabilities of error $\{\mathcal{P}_e(k)\}$, and without channel-coding in subbands. Equation (19) is the **information capacity**, that is, the theoretical upper bound on achievable bit rate with arbitrarily small error. We see that both (17) and (19) depend on the choice of filter bank and are maximized by the PCFB. Suppose the error probabilities are $\mathcal{P}_e(k) = 10^{-7}$ for all k . A calculation of the factor $3/[Q^{-1}(\mathcal{P}_e(k)/2)]^2$ shows that if the two quantities b and \mathcal{C} have to be equal then the total power in (17) should be **9.74 dB** more than the power used in (19). Channel coding is included in many DMT systems in order to reduce this gap.¹¹

¹¹ This gap is very similar to the gap between PCM rate and channel capacity for AWGN channels found in many books on digital communications [35, Chap. 15].

10.5. An Example with Twisted Pairs

The copper twisted pair reaches every home which has a telephone facility. In the earliest days of telephone history the line was used mostly to transmit voice band (up to about 4 kHz). Subsequently however the twisted pair has been used for transmission of digital data as shown by developments such as the ISDN and more recently DSL (digital subscriber loop) services. The data rate achievable on such a line is limited by a number of factors. First there is channel noise and second, the gain of the line $|C(f)|^2$ decreases with frequency and the wire length. The signal-to-noise ratio deteriorates rapidly with frequency as well as wire length. Nevertheless, with typical noise sources of the kind encountered in a DSL environment and with typical transmitted power levels, a wire of length 18 kilofeet could achieve a rate well above 1 Mb/s. Shorter wires (e.g., 1 kft) can achieve much more (40 to 60 Mb/s) [53, 72]. This is done by allocating power and bits into a much wider bandwidth than the traditional voice band.

The types of noise that are really important in a DSL environment are near end cross talk (next) and far end cross talk (fext). These arise because several twisted pairs are typically placed in a single cable and therefore suffer from electromagnetic interference from each other. A great deal of study has been done on this, both theoretical and measurement-based [53, 72]. Assuming that all the pairs in the cable are excited with the same input psd, the power spectra of the next and fext noise sources can be estimated using standard procedures. Figure 18 shows a qualitative example, just to demonstrate these ideas with plots that are reasonably close to what one might expect in practice. Parts (a) and (b) show the transmitted downstream and upstream power distribution for asymmetric DSL or ADSL service.¹² The former occupies a larger bandwidth because downstream ADSL provides for transmission at a much higher rate (several megabits per second) than upstream which offers only a few hundred kilobits per second.¹³ Figure 18c shows a typical plot of the channel gain. The dips are due to the so-called “bridged taps” which are attached to telephone lines in the U.S. for service flexibility. Figure 18d shows the typical power spectra of the next and fext noises. The figure also shows the typical interference on the phone line caused by AM radio waves (560 kHz to 1.6 MHz) and from amateur radio (1.81 to 29.7 MHz, which is outside the standard ADSL band as deployed today). These interferences depend of course on the location of the line, time of the day, and many other varying factors. In any case notice that the overall noise spectrum is far from flat. The ratio of the noise spectrum to the channel gain given by $S_{ee}(f)/|C(f)|^2$ is not monotone; in fact it has several bumps and dips because of the appearances of Figs. 18c and 18d.

As explained in Subsection 10.2, for fixed bit rate and error probability, the total transmitted power is minimized by the PCFB corresponding to the effective power spectrum $S_{ee}(f)/|C(f)|^2$ (or rather a discrete time version). And since $S_{ee}(f)/|C(f)|^2$ is far from being monotone, the PCFB is significantly different from the contiguous brickwall stacking. The reduction in transmitted power could therefore be significant. By using the typical mathematical models for the twisted pair transfer function and the various noise

¹² The downstream signal flows from the telephone office to customer whereas the upstream signal is in the opposite direction. These signals often occupy nonoverlapping bands but sometimes they are in the same band, in which case echo cancellers are required [53].

¹³ The plots represent $10\log P(f)$ where $P(f)$ is the power spectrum in milliwatts per Hertz. The units for $10\log P(f)$ are referred to as dBm/Hz.

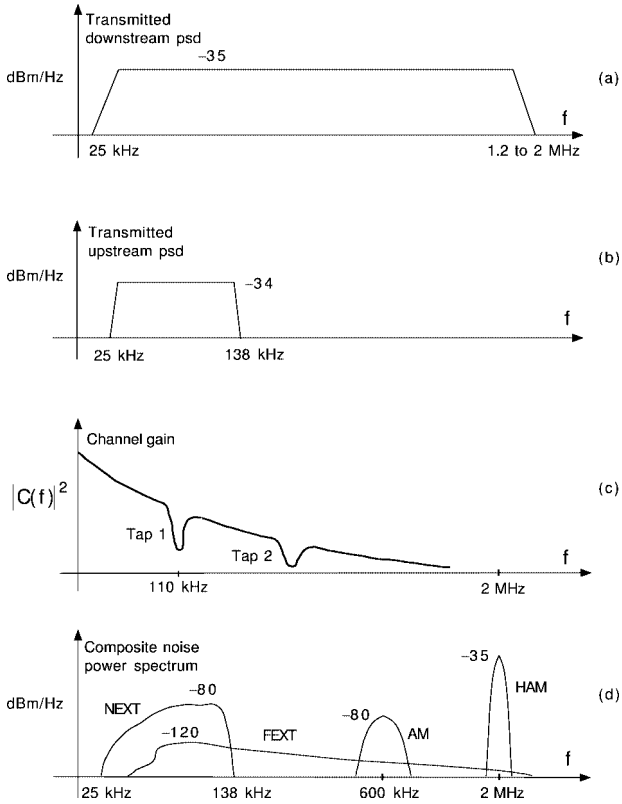


FIG. 18. Qualitative frequency-domain plots pertaining to the ADSL service on the twisted pair copper channel. (a) and (b) The power spectra of the transmitted downstream and upstream signals. (c) The channel gain with two bridged taps. (d) The composite noise psd coming from various sources in the ADSL environment.

sources, we have performed preliminary calculations to demonstrate this difference. For example, assume $M = 16$ and let the probability of error be $\mathcal{P}_e(k) = 10^{-9}$ for all k . Assume further that PAM constellations are to be used. Then for a downstream ADSL bit rate of 3.4 Mb/s, the transmitted power is required to have the values

traditional DFT-multitone	9 mW
ideal FB (contiguous stacking, Fig. 2b)	2.5 mW
ideal PCFB (unconstrained class \mathcal{C}_u)	0.5 mW,

where the PCFB is for the psd $S_{ee}(f)/|C(f)|^2$. Even though the preceding numbers show that the PCFB is attractive for small M , the gap between DFT and ideal PCFB is less impressive for large values such as $M = 512$ typically used in DMT practice. Moreover, the DMT systems based on fixed filter banks such as the DFT or cosine modulated filter banks [13, 51] are attractive because of the efficiency with which they can be implemented. A PCFB solution in general may not lead to such an efficient implementation, even though it is optimal from a performance point of view. Moreover, the PCFB depends on the channel and therefore needs to be adapted. The PCFB yields a useful bound for performance comparisons for fixed number of bands M . If the performance gap between a practical

system and the PCFB solution is small in a particular application, this gives the assurance that we are not very far from optimality.

11. CONCLUDING REMARKS AND OPEN PROBLEMS

A PCFB has so far been shown to exist only for the three classes described in Section 9, namely the two-channel class, the transform coder class \mathcal{C}' , and the unconstrained class \mathcal{C}'' . For the two-channel IIR case, very efficient practical procedures can be found in [57]. For the practical class of FIR orthonormal filter banks, sequential procedures have been described to arrive at suboptimum filter banks (e.g., see [9, 42]), but do not necessarily result in a PCFB for the simple reason that a PCFB does not necessarily exist in these cases! As mentioned earlier, the PCFB has in fact been shown not to exist for certain classes such as DFT filter banks and cosine modulated filter banks, even if the filters are allowed to be of infinite order. It has even been conjectured that the PCFB does not exist (for arbitrary input psd) for classes other than the three mentioned above; this issue remains open at this time.

When a PCFB does not exist, the optimal orthonormal filter bank for one objective function might differ from the solution to another objective, even though both may be concave in the subband variance vector. The procedure to find such filter banks is often ad hoc. Consider M band orthonormal FIR filter banks with filter orders bounded by some integer N . For this class there is no procedure to find the globally optimal FIR orthonormal filter bank to maximize the coding gain, even under high bit-rate assumptions. However, very useful suboptimal methods do exist for such optimization [41, 42]. Theoretical conditions for optimality in the FIR case (analogous to Theorem 1 in the unconstrained case) are not known. For the same reason the connection between optimal compaction filters and optimal coding gain in the FIR case has not been established. An analysis of “sequential compaction algorithms” when PCFBs do not exist is given in [10, Sect. 3.3]. Discussions on optimization of nonuniform filter banks can be found in [8, 36, 65]. The idea of principal component filter banks can be extended to the case of nonuniform filters banks. However, as shown in [8], the optimality properties are not as simple as in the uniform case.

APPENDIX A

Proof of Lemma 1

Imagine that \mathbf{v}_1 can be expressed as a convex combination

$$\mathbf{v}_1 = \sum_{i=1}^J \alpha_i \mathbf{p}_i, \quad \mathbf{p}_i \in \mathcal{P}. \quad (20)$$

Each \mathbf{p}_i is a convex combination of the generating vectors, i.e., $\mathbf{p}_i = \sum_k c_{ik} \mathbf{v}_k$. So $\mathbf{v}_1 = \sum_{k=1}^N (\sum_{i=1}^J \alpha_i c_{ik}) \mathbf{v}_k$. Note that $\sum_{k=1}^N \sum_{i=1}^J \alpha_i c_{ik} = \sum_{i=1}^J \alpha_i \sum_{k=1}^N c_{ik} = \sum_{i=1}^J \alpha_i = 1$. By minimality of $\{\mathbf{v}_k\}$, the vector \mathbf{v}_1 cannot be a convex combination of the other \mathbf{v}_k . So we conclude that $\sum_{i=1}^J \alpha_i c_{ik} = 0$ for $k > 1$. Since $\alpha_i c_{ik} \geq 0$, this means that for each i we have either (a) $\alpha_i = 0$ or (b) $c_{ik} = 0$ for all $k > 1$, that is, $\mathbf{p}_i = \mathbf{v}_1$. So any convex combination (20) reduces to the trivial form $\mathbf{v}_1 = \mathbf{v}_1$ showing that \mathbf{v}_1 is an extreme point.

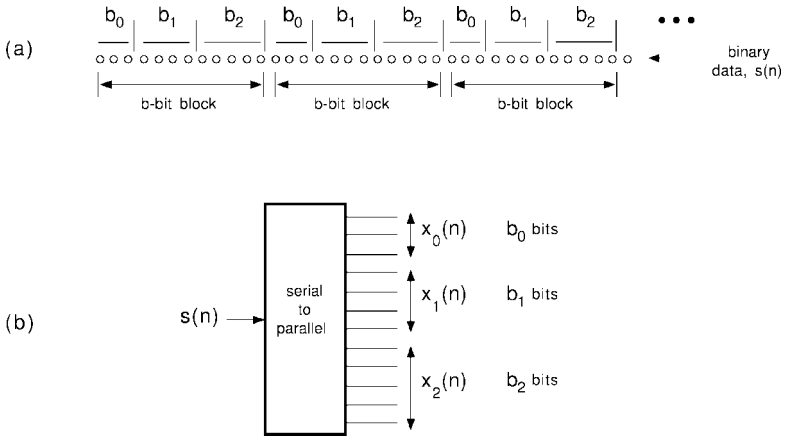


FIG. 19. The parsing stage in multitone modulation. (a) Binary data divided into nonoverlapping b -bit blocks, with each block partitioned into M groups of bits ($M = 3$). (b) The modulation symbols $x_k(n)$ generated from the M groups of bits.

APPENDIX B

The Parsing Stage in DMT Communication

Figure 19a shows the first stage of multitone modulation [11, 13] called the **parsing stage**. Here $s(n)$ represents **binary data** to be transmitted over a channel. These data are divided into nonoverlapping b -bit blocks. The b bits in each block are partitioned into M groups, the k th group being a collection of b_k bits (demonstrated in the figure for $M = 3$). Thus the total number of bits b per block can be expressed as

$$b = \sum_{k=0}^{M-1} b_k.$$

The b_k bits in the k th group constitute the k th symbol x_k which can therefore be regarded as a b_k -bit number. For the n th block, this symbol is denoted as $x_k(n)$. We

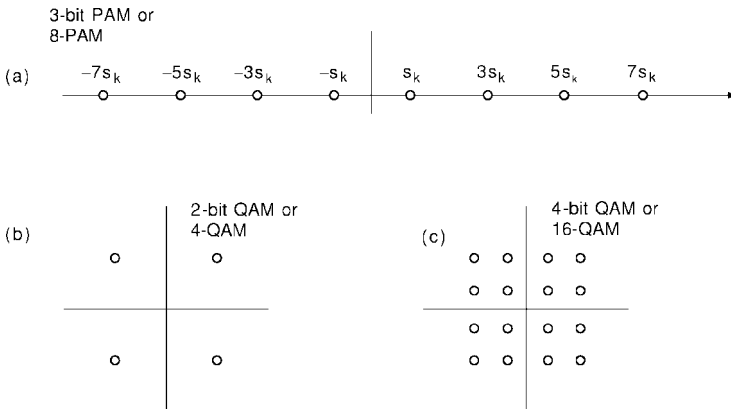


FIG. 20. Examples of PAM and rectangular QAM constellations for DMT. (a) The 8-PAM constellation (3 bits), (b) the 4-QAM constellation (2 bits), and (c) the 16-QAM constellation (4 bits).

shall refer to $x_k(n)$ as the *modulation symbol* for the k th band. For the case of pulse amplitude modulation (PAM), the sample $x_k(n)$ is a quantized real number as demonstrated in Fig. 20a for $b_k = 3$. For the case of quadrature amplitude modulation (QAM) $x_k(n)$ can be regarded as a complex number, taking one of 2^{b_k} possible values from a constellation as demonstrated in Figs. 20b and 20c.¹⁴ The advantage of QAM is that it allows more efficient use of available bandwidth by multiplexing two messages in the same two sided bandwidth [49]. The QAM constellations shown in Figs. 20b and 20c are called rectangular constellations. More efficient constellations exist (see [49] and references therein) but rectangular constellations are commonly used because of their simplicity. In this paper we shall restrict most of our discussions to the case of PAM.

ACKNOWLEDGMENT

The authors thank Dr. Henrique Malvar of Microsoft Research for the kind invitation to write this article. Very useful comments from the reviewers are also gratefully acknowledged.

REFERENCES

1. K. C. Aas and C. T. Mullis, Minimum mean-squared error transform coding and subband coding, *IEEE Trans. Inform. Theory* July (1996), 1179–1192.
2. S. O. Aase and T. Ramstad, On the optimality of nonunitary filter banks in subband coders, *IEEE Trans. Image Process.* December (1995), 1585–1591.
3. A. N. Akansu, P. Duhamel, X. Lin, and M. de Courville, Orthogonal transmultiplexers in communications: A review, *IEEE Trans. Signal Process.* April (1998), 979–995.
4. A. N. Akansu and R. A. Haddad, “Multiresolution Signal Decomposition: Transforms, Subbands, and Wavelets,” Academic Press, San Diego, 1992.
5. A. N. Akansu and Y. Liu, On signal decomposition techniques, *Opt. Engrg.* **30** (1991), 912–920.
6. S. Akkarakaran and P. P. Vaidyanathan, On optimization of filter banks with denoising applications, in “Proc. IEEE ISCAS, Orlando, FL, June 1999.”
7. S. Akkarakaran and P. P. Vaidyanathan, The role of principal component filter banks in noise reduction, in “Proc. SPIE, Denver, CO, July 1999.”
8. S. Akkarakaran and P. P. Vaidyanathan, On nonuniform principal component filter banks: Definitions, existence and optimality, in “Proc. SPIE, San Diego, CA, July 2000.”
9. S. Akkarakaran and P. P. Vaidyanathan, Filter bank optimization with convex objectives, and the optimality of principal component forms, *IEEE Trans. Signal Process.* January (2001), 100–114.
10. S. Akkarakaran and P. P. Vaidyanathan, Results on principal component filter banks: Colored noise suppression and existence issues, *IEEE Trans. Inform. Theory* March (2001).
11. J. A. C. Bingham, Multicarrier modulation for data transmission: An idea whose time has come, *IEEE Comm. Mag.* May (1990), 5–14.
12. G. Cherubini, E. Eleftheriou, S. Olcer, and J. M. Cioffi, Filter bank modulation techniques for very high speed digital subscriber lines, *IEEE Comm. Mag.* May (2000), 98–104.
13. J. S. Chow, J. C. Tu, and J. M. Cioffi, A discrete multitone transreceiver system for HDSL applications, *IEEE J. Selected Areas Comm.* August (1991), 895–908.
14. T. M. Cover and J. A. Thomas, “Elements of Information Theory,” Wiley, New York, 1991.
15. S. Dasgupta, C. Schwarz, and B. D. O. Anderson, Optimum subband coding of cyclostationary signals, in “Proc. IEEE Int. Conf. Acoust. Speech and Sig. Proc., Phoenix, 1999,” pp. 1489–1492.

¹⁴ Notice that b_k -bit signals are also referred to as M_k -ary signals where $M_k = 2^{b_k}$. Thus 3-bit PAM is the same as 8-ary PAM, 4-bit QAM the same as 16-ary QAM, and so forth.

16. R. L. de Queiroz and H. S. Malvar, On the asymptotic performance of hierarchical transforms, *IEEE Trans. Signal Process.* **40** (1992), 2620–2622.
17. I. Djokovic and P. P. Vaidyanathan, On optimal analysis/synthesis filters for coding gain optimization, *IEEE Trans. Signal Process.* May (1996), 1276–1279.
18. D. L. Donoho and I. M. Johnstone, Ideal spatial adaptation by wavelet shrinkage, *Biometrika* **81** (1994), 425–455.
19. T. R. Fischer, On the rate-distortion efficiency of subband coding, *IEEE Trans. Inform. Theory* **38** (1992), 426–428.
20. J. L. Franklin, “Methods of Mathematical Economics,” Springer-Verlag, New York, 1980.
21. A. Gersho and R. M. Gray, “Vector Quantization and Signal Compression,” Kluwer Academic, Dordrecht, 1992.
22. R. A. Gopinath, J. E. Odegard, and C. S. Burrus, Optimal wavelet representation of signals and the wavelet sampling theorem, *IEEE Trans. Circuits Systems* April (1994), 262–277.
23. R. A. Haddad and N. Uzun, Modeling, analysis, and compensation of quantization effects in M -band subband codecs, in “Proc. IEEE Int. Conf. Acoust. Speech and Sig. Proc., Minneapolis, 1993,” pp. 173–176.
24. A. Hjørungnes and T. A. Ramstad, Jointly optimal analysis and synthesis filter banks for bit-constrained source coding, in “Proc. IEEE ICASSP, Seattle, WA, May 1998,” pp. 1337–1340.
25. A. Hjørungnes, H. Coward, and T. A. Ramstad, Minimum mean square error FIR filter banks with arbitrary filter lengths, in “Proc. Int. Conf. Image Proc., Kobe, Japan, Oct. 1999,” pp. 619–623.
26. R. A. Horn and C. R. Johnson, “Matrix Analysis,” Cambridge Univ. Press, Cambridge, UK, 1985.
27. Y. Huang and P. M. Schultheiss, Block quantization of correlated Gaussian random variables, *IEEE Trans. Comm. Syst.* September (1963), 289–296.
28. N. S. Jayant and P. Noll, “Digital Coding of Waveforms,” Prentice Hall, Englewood Cliffs, NJ, 1984.
29. I. Kalet, The multitone channel, *IEEE Trans. Comm.* February (1989), 119–124.
30. I. Kalet, Multitone modulation, in “Subband and Wavelet Transforms” (A. N. Akansu and M. J. Smith, Eds.), Kluwer Academic, Dordrecht, 1996.
31. A. Kirac and P. P. Vaidyanathan, On existence of FIR principal component filter banks, in “IEEE Int. Conf. ASSP, Seattle, 1998.”
32. A. Kirac and P. P. Vaidyanathan, Optimality of orthonormal transforms for subband coding, in “IEEE DSP Workshop, Utah, 1998.”
33. A. Kirac and P. P. Vaidyanathan, Theory and design of optimum FIR compaction filters, *IEEE Trans. Signal Process.* April (1998), 903–919.
34. R. D. Koilpillai, T. Q. Nguyen, and P. P. Vaidyanathan, Some results in the theory of cross talk free transmultiplexers, *IEEE Trans. Signal Process.* October (1991), 2174–2183.
35. B. P. Lathi, “Modern Digital and Analog Communication Systems,” Oxford Univ. Press, London, 1998.
36. Y.-P. Lin and P. P. Vaidyanathan, Considerations in the design of optimum compaction filters for subband coders, in “Proc. Eusipco, Trieste, Italy, 1996.”
37. X. Lin and A. N. Akansu, A distortion analysis and optimal design of orthonormal basis for DMT receivers, in “Proc. IEEE ICASSP, 1996,” pp. 1475–1478.
38. Y.-P. Lin and S.-M. Phoong, Optimal DMT transreceivers over fading channels, in “Proc. IEEE ICASSP, Phoenix, AZ, 1999,” pp. 1397–1400.
39. S. Mallat, “A Wavelet Tour of Signal Processing,” Academic Press, San Diego, 1998.
40. H. S. Malvar, “Signal Processing with Lapped Transforms,” Artech House, Norwood, MA, 1992.
41. H. S. Malvar and D. H. Staelin, The LOT: Transform coding without blocking effects, *IEEE Trans. Acoust. Speech Signal Process.* **37** (1989), 553–559.
42. P. Moulin, A new look at signal-adapted QMF bank design, in “Proc. Int. Conf. ASSP, Detroit, May 1995,” pp. 1312–1315.

43. P. Moulin and M. K. Mihcak, Theory and design of signal adapted FIR paraunitary filter banks, *IEEE Trans. Signal Process.* **46** (1998), 920–929.
44. P. Moulin, M. Anitescu, and K. Ramchandran, Theory of rate-distortion optimal, constrained filter banks—Applications to IIR and FIR biorthogonal designs, *IEEE Trans. Signal Process.* **48** (2000), 1120–1132.
45. A. N. Netravali and B. G. Haskell, “Digital Pictures: Representation, Compression, and Standards,” Plenum, New York, 1995.
46. S. Ohno and H. Sakai, Optimization of filter banks using cyclostationary spectral analysis, *IEEE Trans. Signal Process.* November (1996), 2718–2725.
47. A. V. Oppenheim and R. W. Schaffer, “Discrete-Time Signal Processing,” Prentice Hall, Englewood Cliffs, NJ, 1999.
48. T. Painter and A. Spanias, Perceptual coding of digital audio, in “Proc. of the IEEE, April 2000,” pp. 451–513.
49. J. G. Proakis, “Digital Communications,” McGraw-Hill, New York, 1995.
50. R. P. Rao and W. A. Pearlman, On entropy of pyramid structures, *IEEE Trans. Inform. Theory* **37** (1991), 407–413.
51. A. D. Rizos, J. G. Proakis, and T. Q. Nguyen, Comparison of DFT and cosine modulated filter banks in multicarrier modulation, in “Proc. of Globecom, Nov. 1994,” pp. 687–691.
52. A. Segall, Bit allocation and encoding for vector sources, *IEEE Trans. Inform. Theory* March (1976), 162–169.
53. T. Starr, J. M. Cioffi, and P. J. Silverman, “Understanding DSL Technology,” Prentice Hall, Englewood Cliffs, NJ, 1999.
54. M. G. Strintzis, Optimal pyramidal and subband decompositions for hierarchical coding of noisy and quantized images, *IEEE Trans. Image Process.* February (1998), 155–166.
55. A. H. Tewfik, D. Sinha, and P. E. Jorgensen, On the optimal choice of a wavelet for signal representation, *IEEE Trans. Inform. Theory* March (1992), 747–765.
56. M. K. Tsatsanis and G. B. Giannakis, Principal component filter banks for optimal multiresolution analysis, *IEEE Trans. Signal Process.* **43** (1995), 1766–1777.
57. J. Tuqan and P. P. Vaidyanathan, Optimum low cost two channel IIR orthonormal filter bank, in “Proc. IEEE Int. Conf. Acoust. Speech, and Signal Proc., Munich, April 1997.”
58. J. Tuqan and P. P. Vaidyanathan, A state space approach to the design of globally optimal FIR energy compaction filters, *IEEE Trans. Signal Process.* October (2000), 2822–2838.
59. M. A. Tzannes, M. C. Tzannes, J. G. Proakis, and P. N. Heller, DMT systems, DWMT systems, and digital filter banks, in “Proc. ICC, 1994,” pp. 311–315.
60. M. Unser, On the optimality of ideal filters for pyramid and wavelet signal approximation, *IEEE Trans. Signal Process.* **41** (1993), 3591–3596.
61. M. Unser, An extension of the KLT for wavelets and perfect reconstruction filter banks, in “Proc. SPIE No. 2034, Wavelet Appl. in Signal and Image Proc., San Diego, CA, 1993,” pp. 45–56.
62. P. P. Vaidyanathan, “Multirate Systems and Filter Banks,” Prentice Hall, Englewood Cliffs, NJ, 1993.
63. P. P. Vaidyanathan, Orthonormal and biorthogonal filter-banks as convolvers, and convolutional coding gain, *IEEE Trans. Signal Process.* **41** (1993), 2110–2130.
64. P. P. Vaidyanathan and T. Chen, Statistically optimal synthesis banks for subband coders, in “Proc. Asilomar Conference on Signals, Systems, and Computers, Monterey, CA, Nov. 1994.”
65. P. P. Vaidyanathan, Review of recent results on optimal orthonormal subband coders, in “Proc. SPIE 97, San Diego, July 1997.”
66. P. P. Vaidyanathan, Theory of optimal orthonormal subband coders, *IEEE Trans. Signal Process.* **46** (1998), 1528–1543.
67. P. P. Vaidyanathan and A. Kirac, Results on optimal biorthogonal filter banks, *IEEE Trans. Circuits Systems* (1998), 932–947.
68. P. P. Vaidyanathan, Y.-P. Lin, S. Akkarakaran, and S.-M. Phoong, Optimality of principal component filter banks for discrete multitone communication systems, in “Proc. IEEE ISCAS, Geneva, May 2000.”

69. P. P. Vaidyanathan and S. Akkarakaran, A Review of the Theory and Applications of Principal Component Filter Banks, Technical Report, California Institute of Technology, Pasadena, CA, June 2000.
70. M. Vetterli, Perfect transmultiplexers, in "Proc. ICASSP, 1986," pp. 2567–2570.
71. M. Vetterli and J. Kovačević, "Wavelets and Subband Coding," Prentice Hall, Englewood Cliffs, NJ, 1995.
72. J.-J. Werner, The HDSL environment, *IEEE J. Sel. Areas Comm.* **9** (1991), 785–800.
73. B. Xuan and R. H. Bamberger, FIR principal component filter banks, *IEEE Trans. Signal Process.* April (1998), 930–940.